Lidar Technique: Basic Hardware Components (Lasers and Electronics)

Prof. Dr. Alex Papayannis

Head of the Laser Remote Sensing Unit (LRSU)

National Technical University of Athens, Greece

Website: http://lrsu.physics.ntua.gr/en

Email: apdlidar@central.ntua.gr

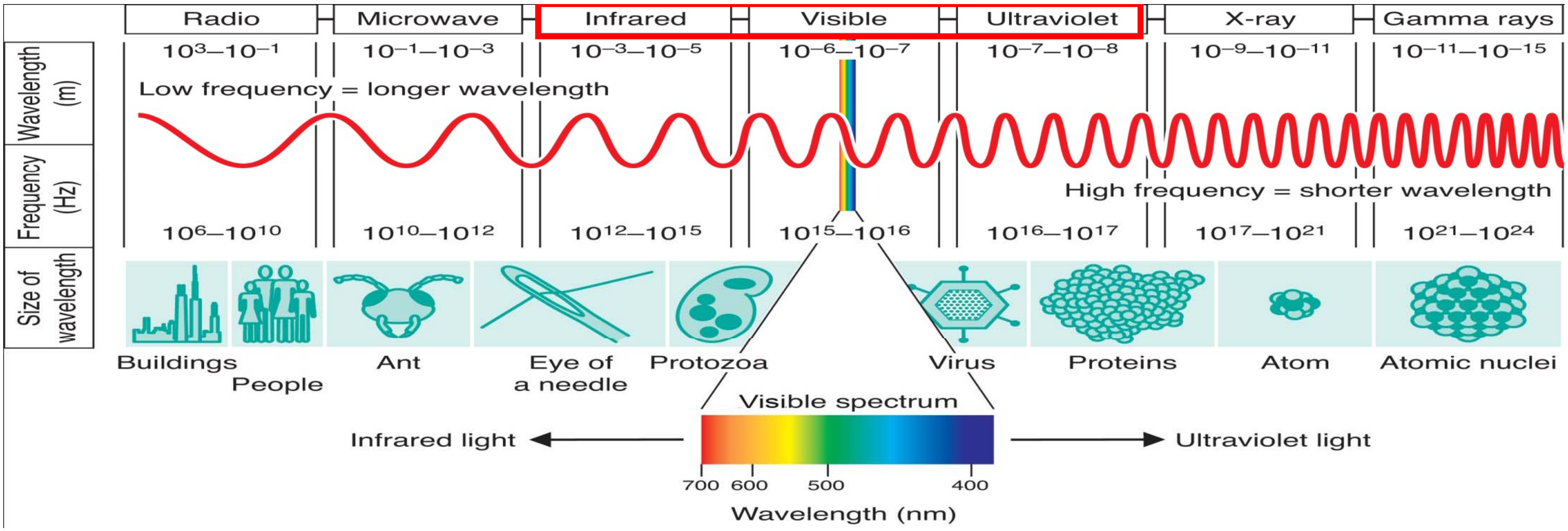
Radio
Microwave
Infrared
Visible
Ultraviolet
X-ray
Gamma rays
Wavelength (m)
10^3–10^-1
10^-1–10^-3
10^-3–10^-5
10^-6–10^-7
10^-7–10^-8
10^-9–10^-11
10^-11–10^-15
Low frequency = longer wavelength
High frequency = shorter wavelength
Frequency (Hz)
10^6–10^10
10^10–10^12
10^12–10^15
10^15–10^16
10^16–10^17
10^17–10^21
10^21–10^24
Size of wavelength
Buildings
People
Ant
Eye of a needle
Protozoa
Virus
Proteins
Atom
Atomic nuclei
Visible spectrum
Infrared light
Ultraviolet light
700 600 500 400
Wavelength (nm)

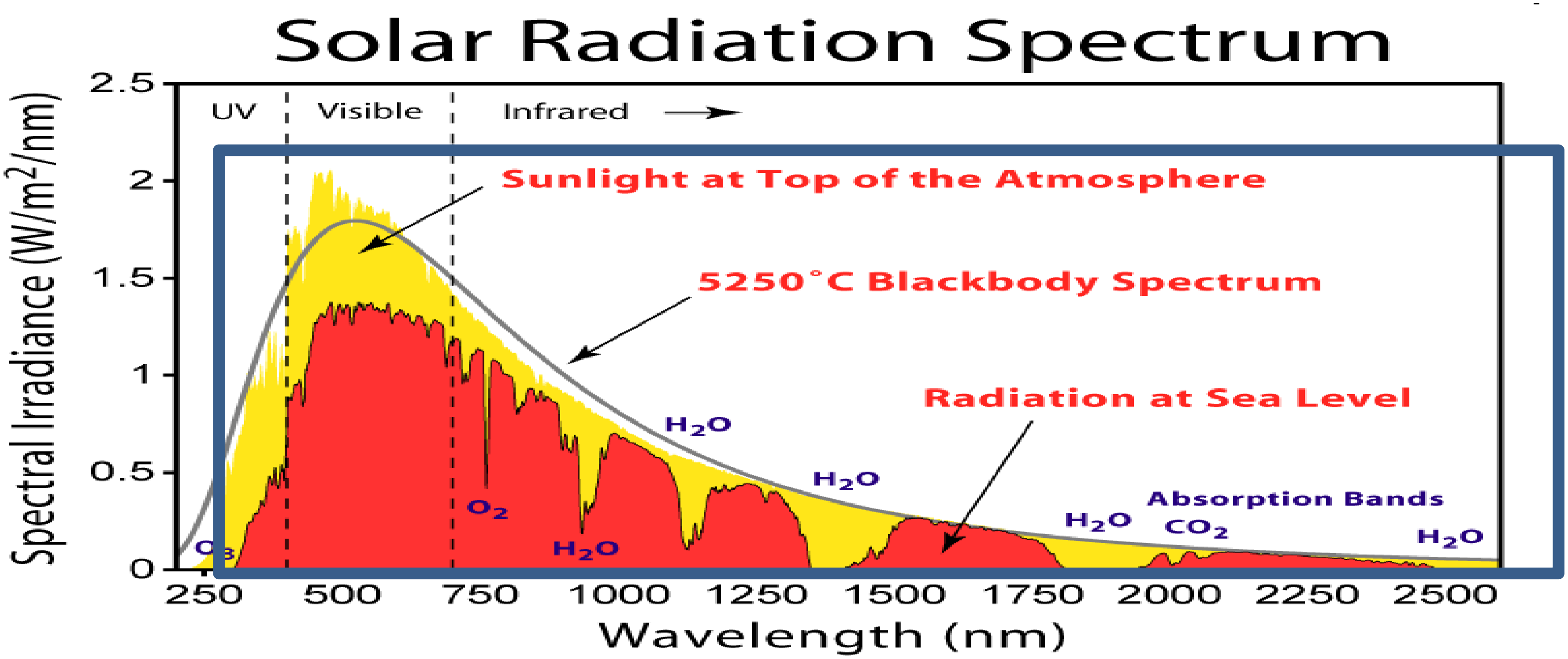
Solar Radiation Spectrum
Spectral Irradiance (W/m²/nm)
2.5
2
1.5
1
0.5
0
UV
Visible
Infrared
Sunlight at Top of the Atmosphere
5250°C Blackbody Spectrum
Radiation at Sea Level
H₂O
H₂O
O₂
H₂O
H₂O
Absorption Bands
CO₂
H₂O
O₃
250 500 750 1000 1250 1500 1750 2000 2250 2500
Wavelength (nm)

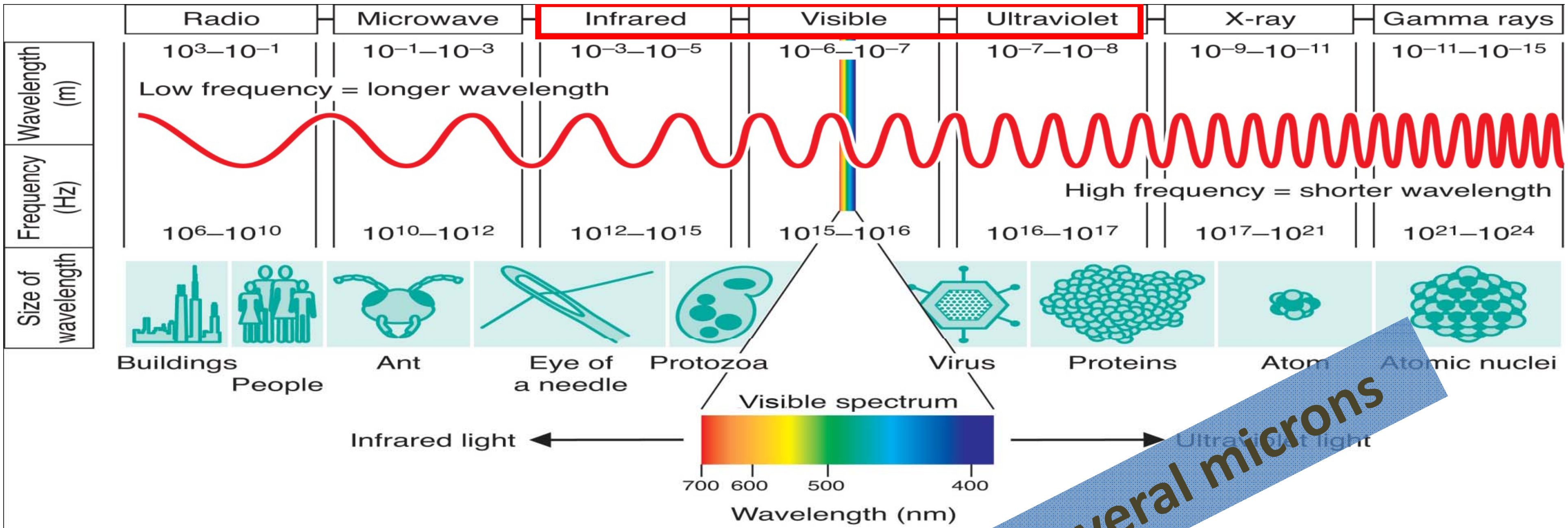

Lidars: from around 260 nm → several microns

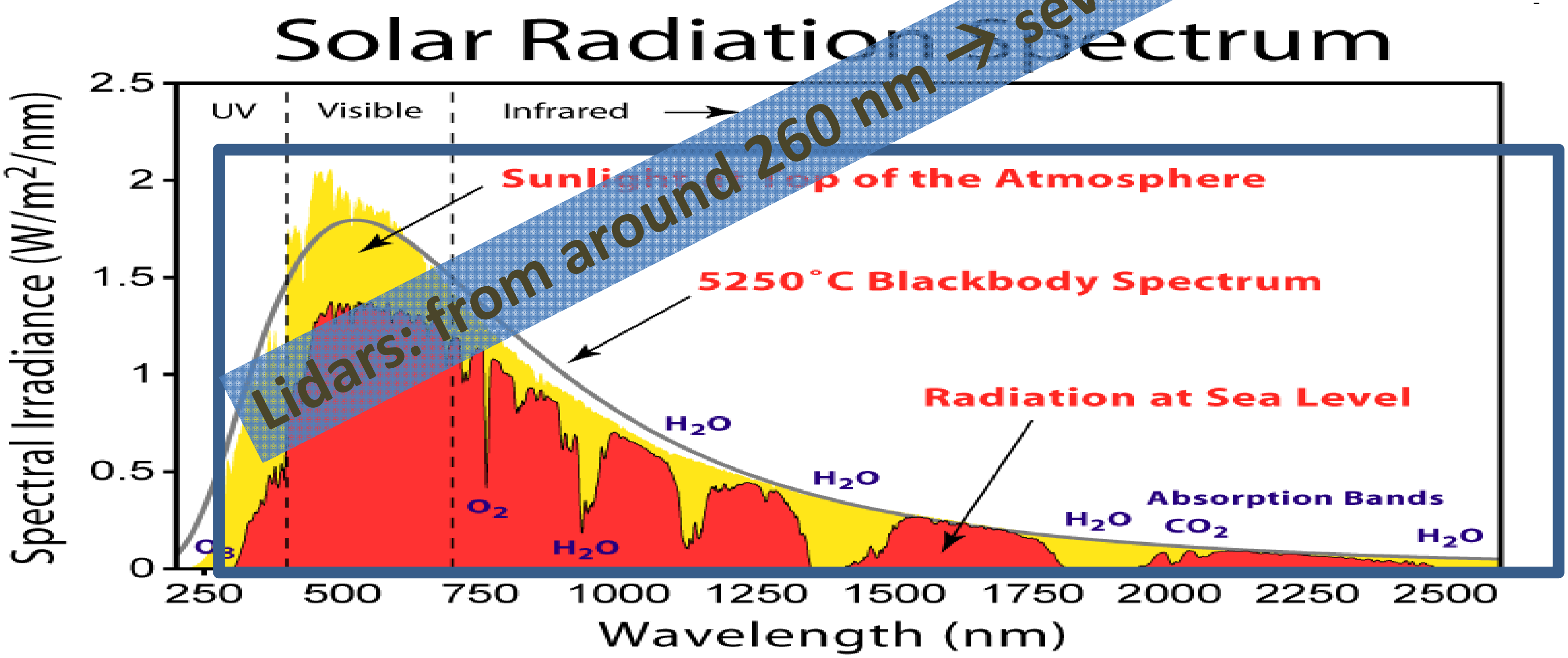

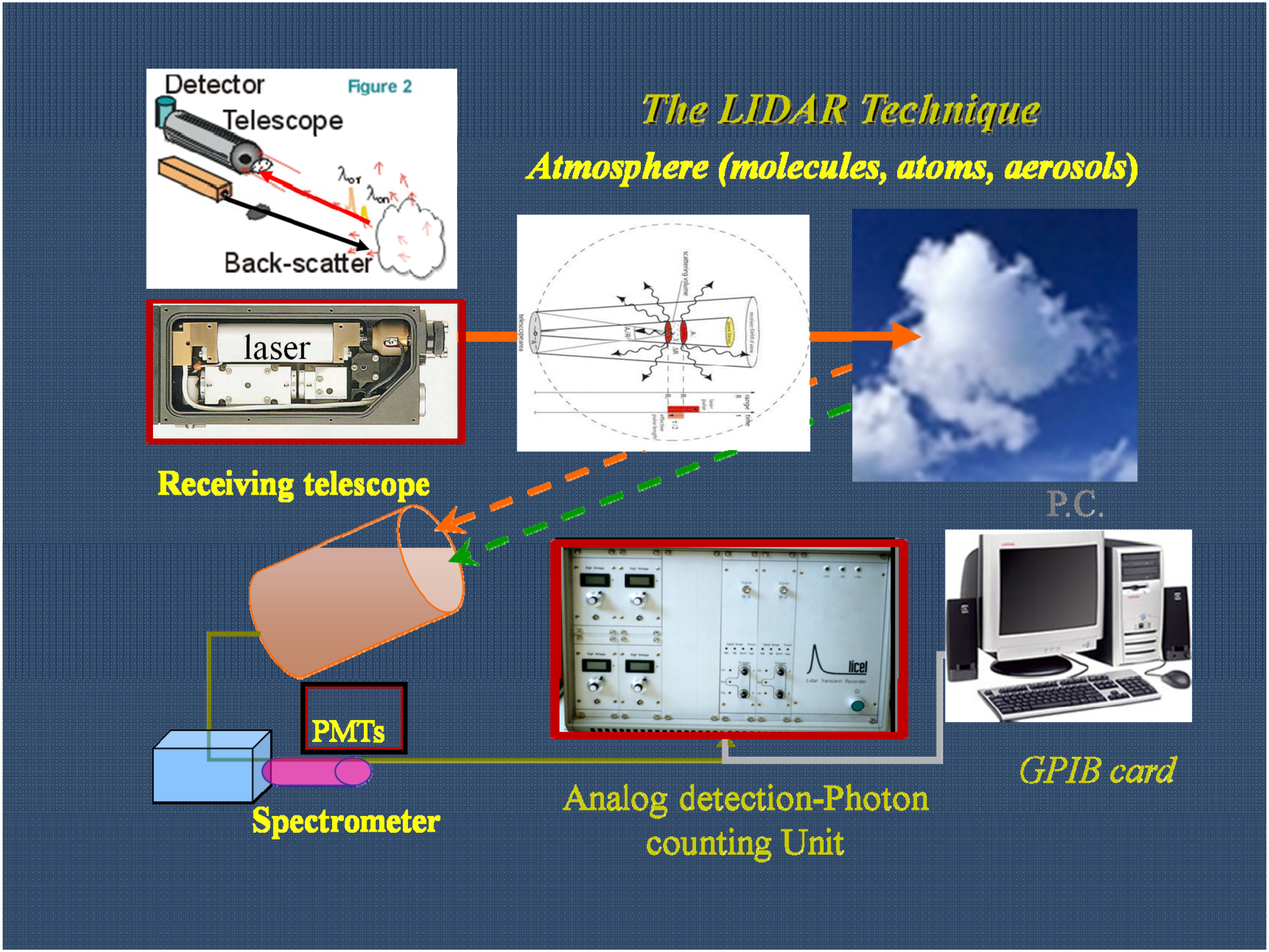
The LIDAR Technique
Atmosphere (molecules, atoms, aerosols)
Detector
Figure 2
Telescope
Back-scatter
laser
Receiving telescope
P.C.
PMTs
Spectrometer
Analog detection-Photon counting Unit
GPIB card
licel
Lidar Transient Recorder

Typical LIDAR Experimental Set-up

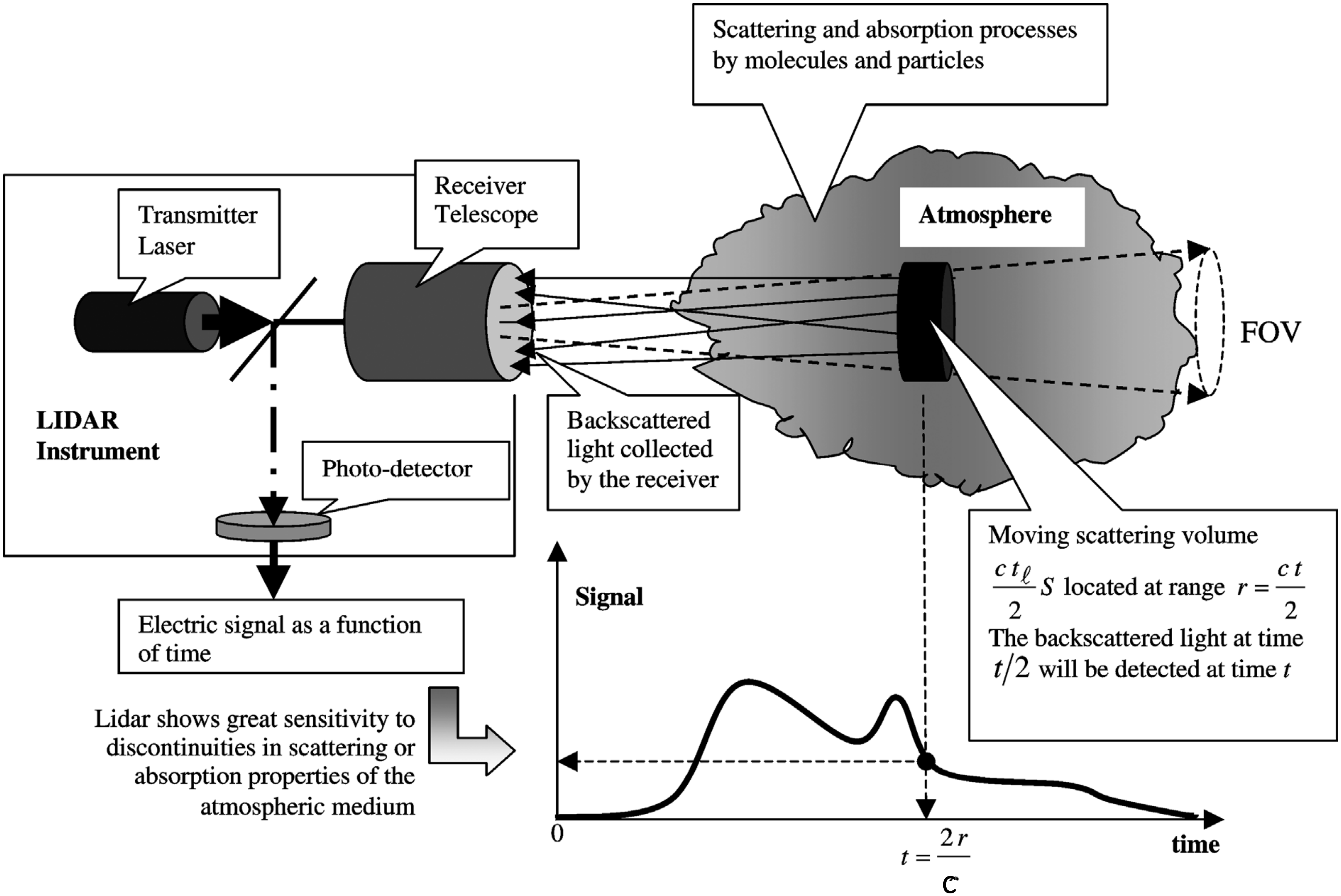

The Lidar Principle

$\Delta t^* = 1/F_D$, F_D=Signal sampling frequency (10-40 MHz→~GHz), Δz=range resolution

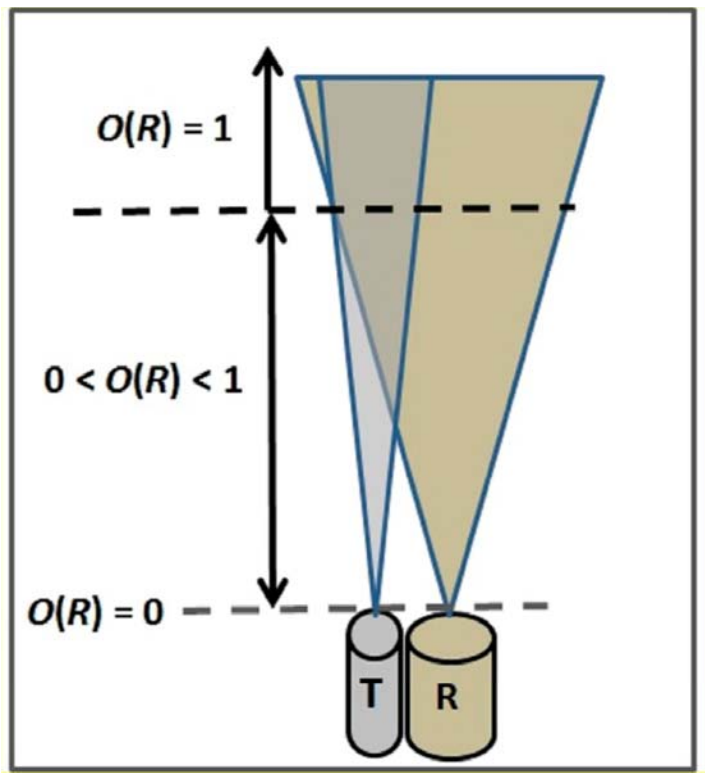

$$\Delta z = c\,(\Delta t^*)/2$$

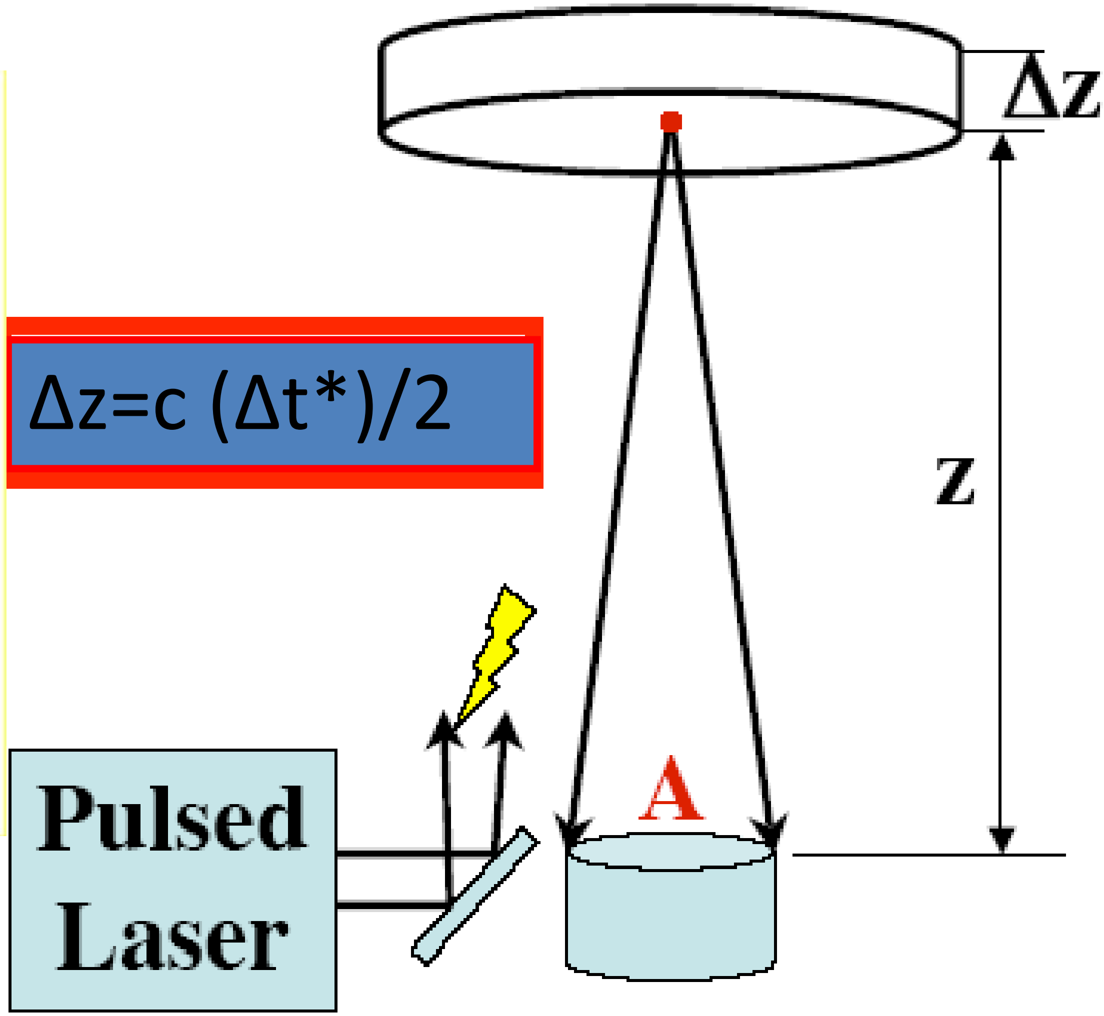

O(R): Overlap function
T: Laser (Emitter)
R: Telescope (Receiver)

[Pal, S., Remote Sensing, 6, 8468-8493, 2014]

Lidar signal $S(z) \sim 1/z^2$

Lidar System Components

General physical properties:

-LIDAR: robust, compact, low power consumption, stability (alignment/optics/mechanical structure), low weight (airborne/space borne systems), easy to operate, 24/7 operationality, remote control, low-cost maintenance-operation,

-Housing: temperature-humidity controlled housing, compact with protection window, indirect solar radiation, weather-proof,

-Transportable (special campaigns).

Transmitter (Laser):

-Single-wavelength & polarized laser beam

- High energy laser source

-Wavelength: 0.266-10.6 um (several wavelengths - tunable for special cases)

- High repetition rates (desired): several Hz to 20 some kHz.

Safety (laser Beam):

Eye-safe emission (exiting the protective window): Use convenient wavelengths + beam expander!

Operation Mode:

-Day/nighttime, continuous, automated operation

-Time resolution (several seconds to minutes)

- Spatial resolution (~15-100 m or better, depending on height)

Signal Received:

- Backscatter (molecules + aerosols)
- Atmospheric Background correction (averaged signal at high ranges)
- Electronic noise evaluation (use of pre-trigger)
- Depolarization channels

Lidar System Components

Laser Sources:

Typical laser sources: Nd:YAG (1.064um), XeCl (0.308um), Er:glass (1.54um), Er:YAG (2.94um), Tm,Ho:YAG (2um), CO_2 (10.6 um), etc.

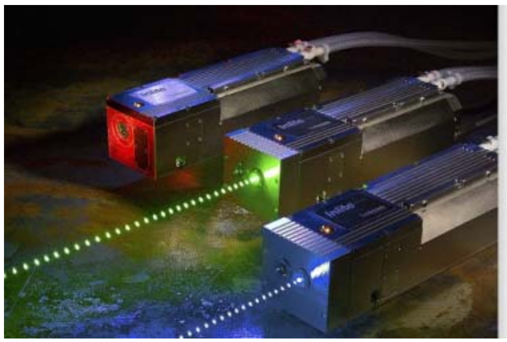

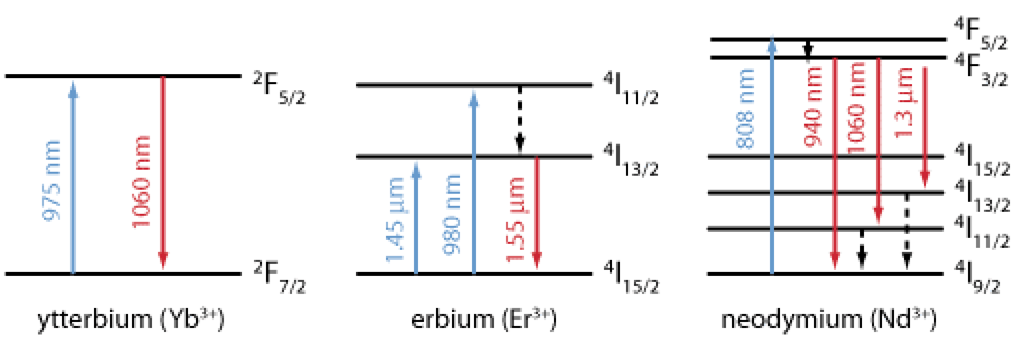

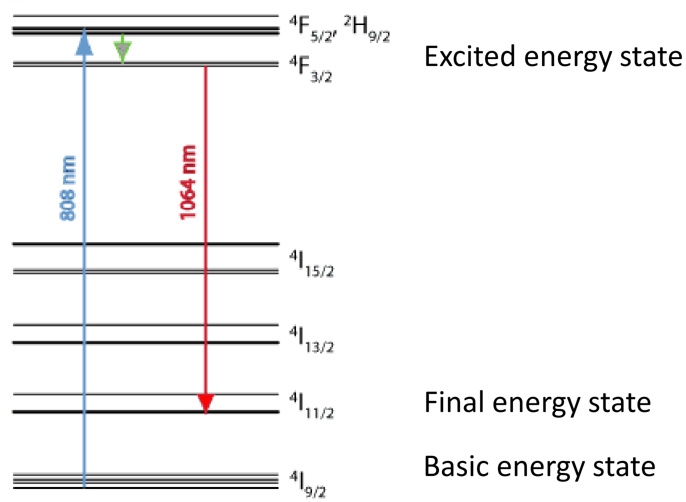

Blue: Pump optical beam (diode laser or flash lamp) **Red:** emitted laser beam

Lidar System Components

Laser Sources:

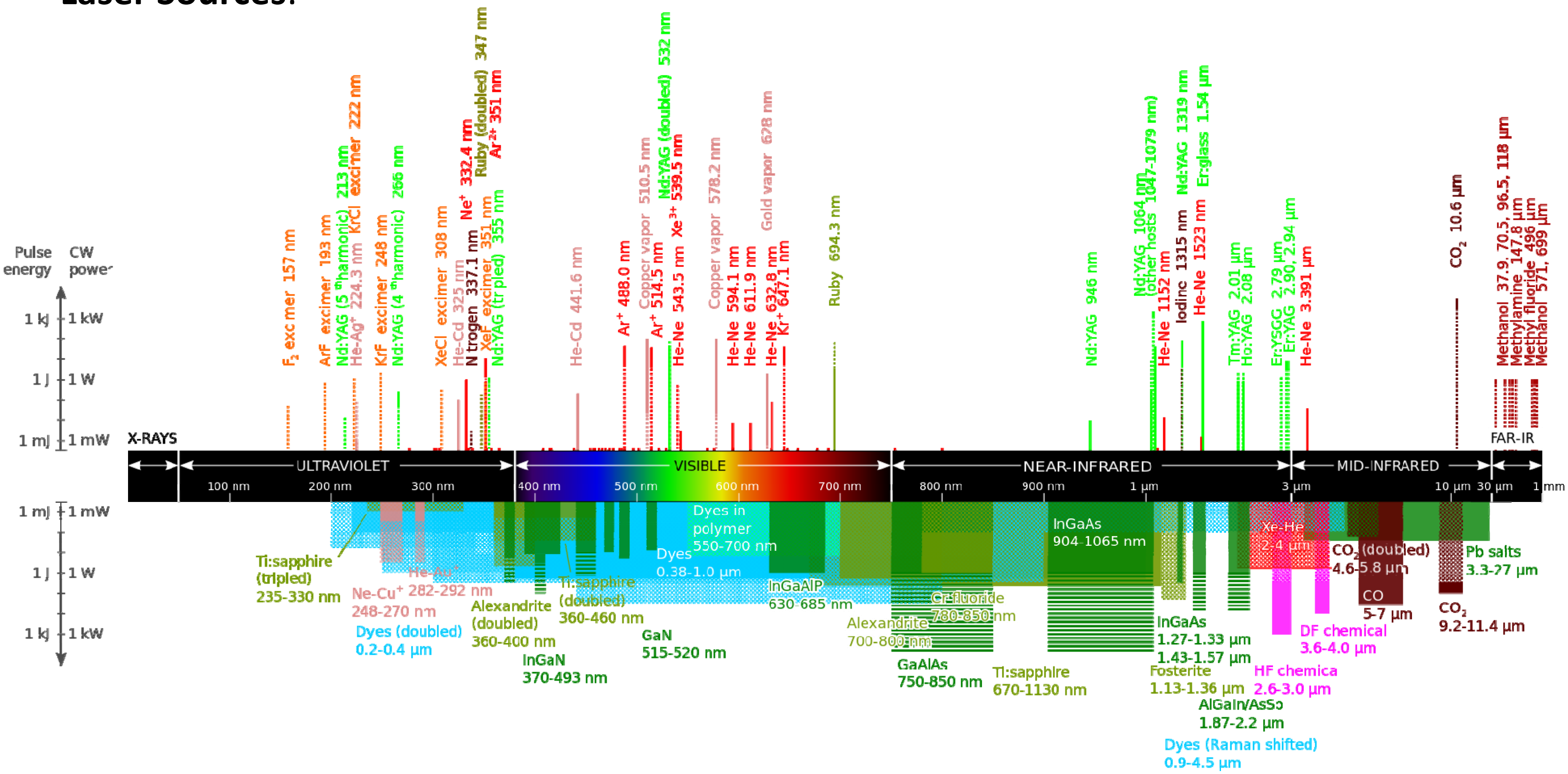

https://en.wikipedia.org/wiki/List_of_laser_types

Lidar System Components

Laser Cavity (Type I-Solid state):

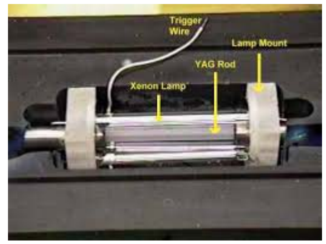

Laser crystals

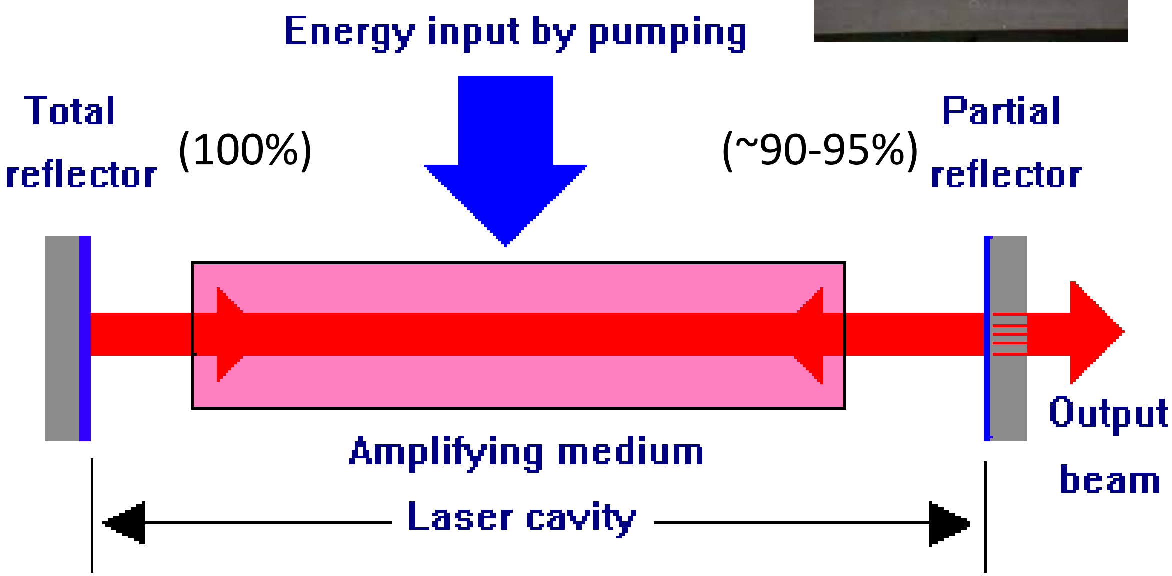

Nanosecond pulses
Up to several Joules/pulse

Cavity reflectors

Lidar System Components

Laser Cavity (Type I-Solid state):

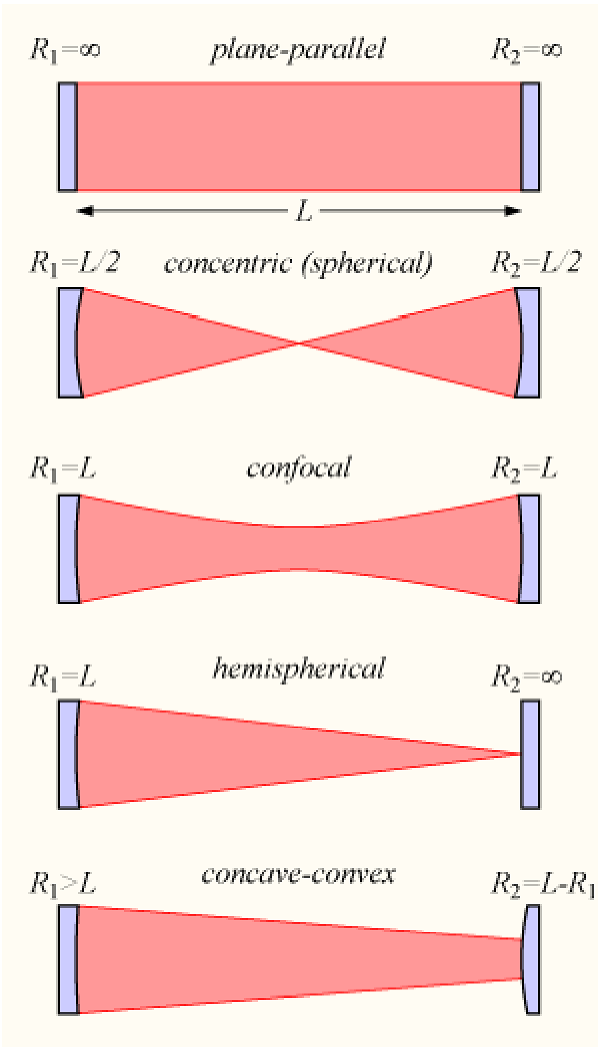

(Stability criterion)

$$0 \leqslant \left(1-\frac{L}{R_1}\right)\left(1-\frac{L}{R_2}\right) \leqslant 1.$$

$$g_1 = 1 - \frac{L}{R_1}, \qquad g_2 = 1 - \frac{L}{R_2}$$

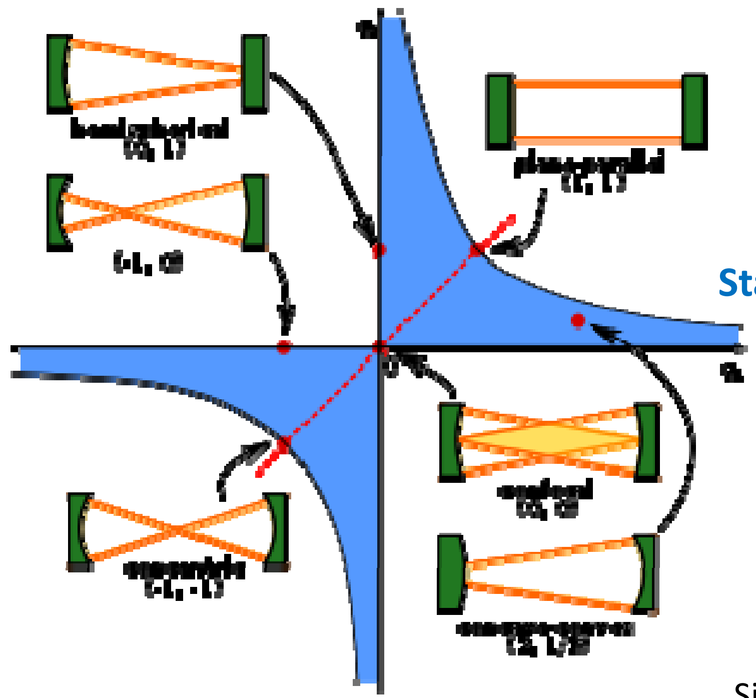

Stability region

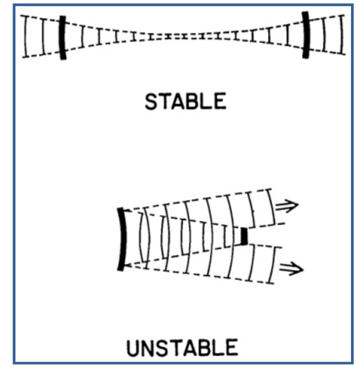

Unstable:
After several round-trips the laser beams largely diverges

Siegman (1986)

Lidar System Components

Laser Cavity (Type IA-Diode pumped solid state lasers):

(100%) (~90-95%)

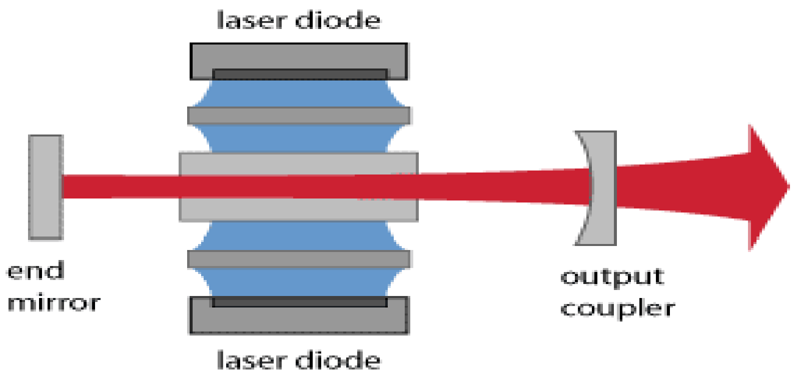

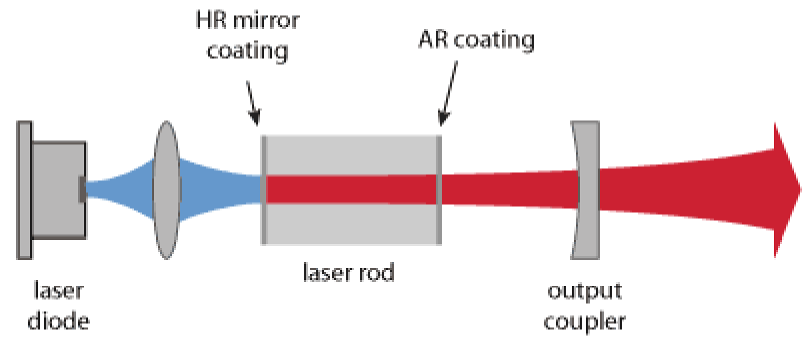

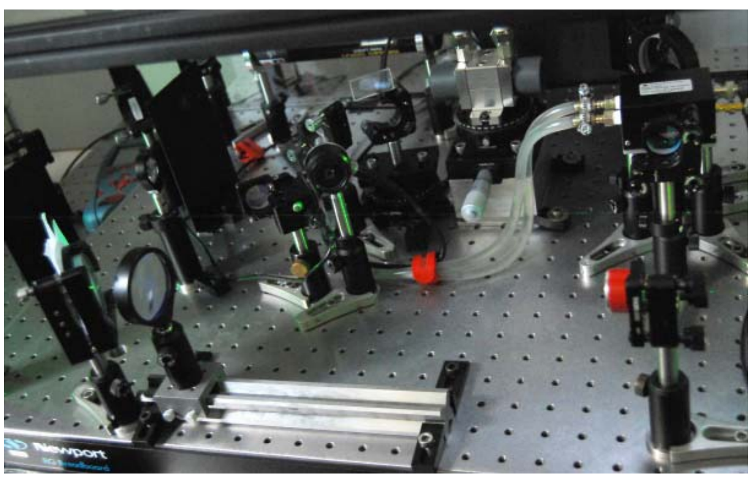

Nanosecond pulses
Up to several Joules/pulse

Diode pumped multi-segmented Nd:YAG laser developed for European Space Agency @ NTUA

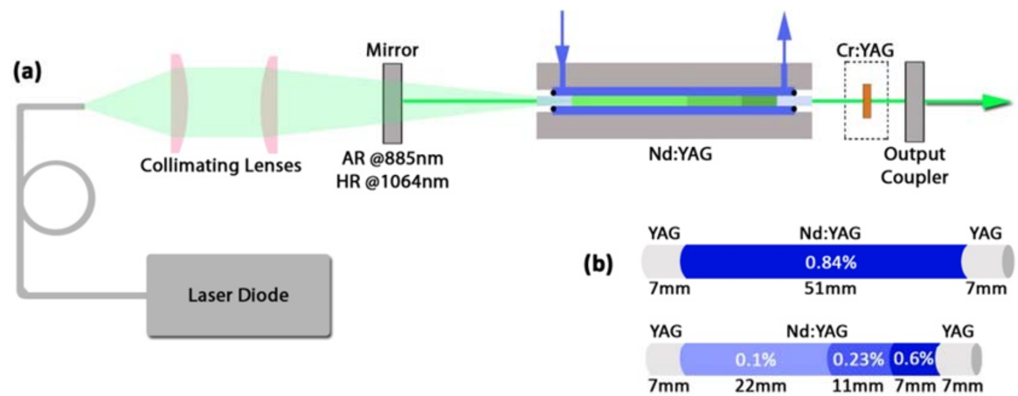

Evangellatos et al. (2013; 2014)

Lidar System Components

Laser Cavity:

Typical laser cavities: (multiple beams passages between 100% reflection mirrors and output couplers)

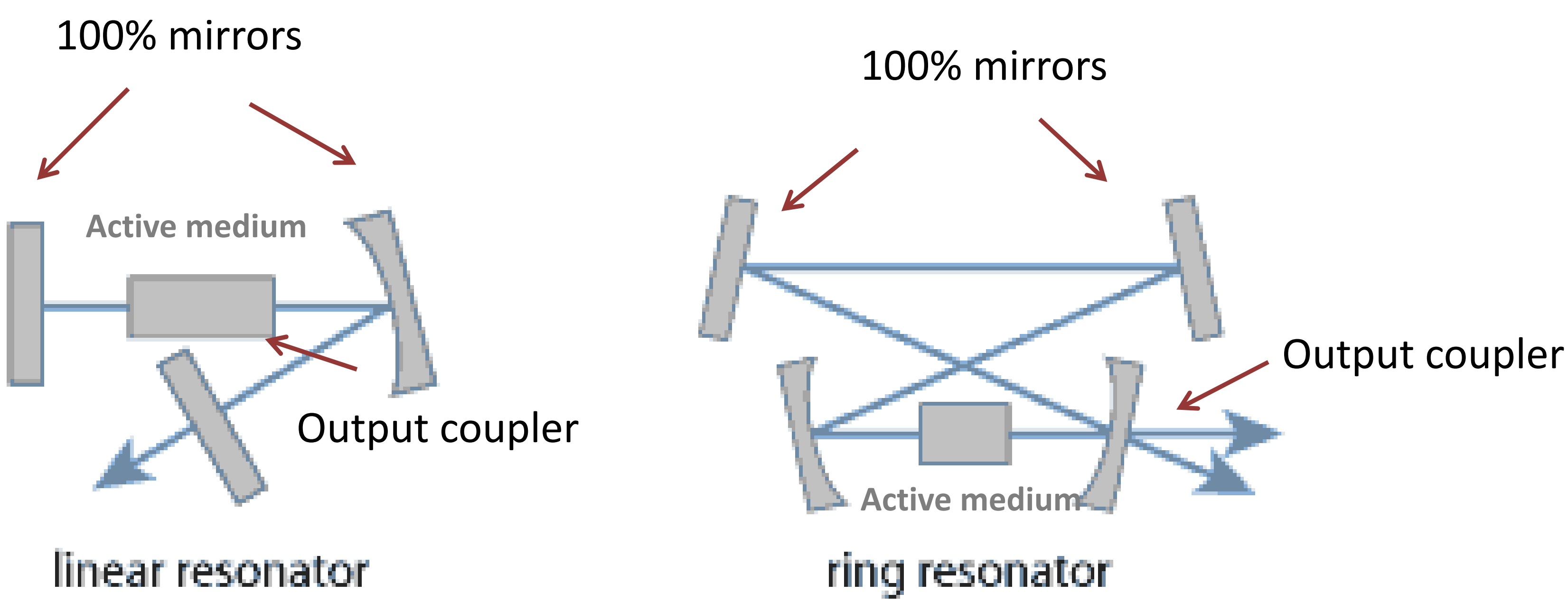

www.rp-photonics.com

Lidar System Components

Laser Cavity:

Typical laser cavities: (multiple beams passages between 100% reflection mirrors and output couplers)

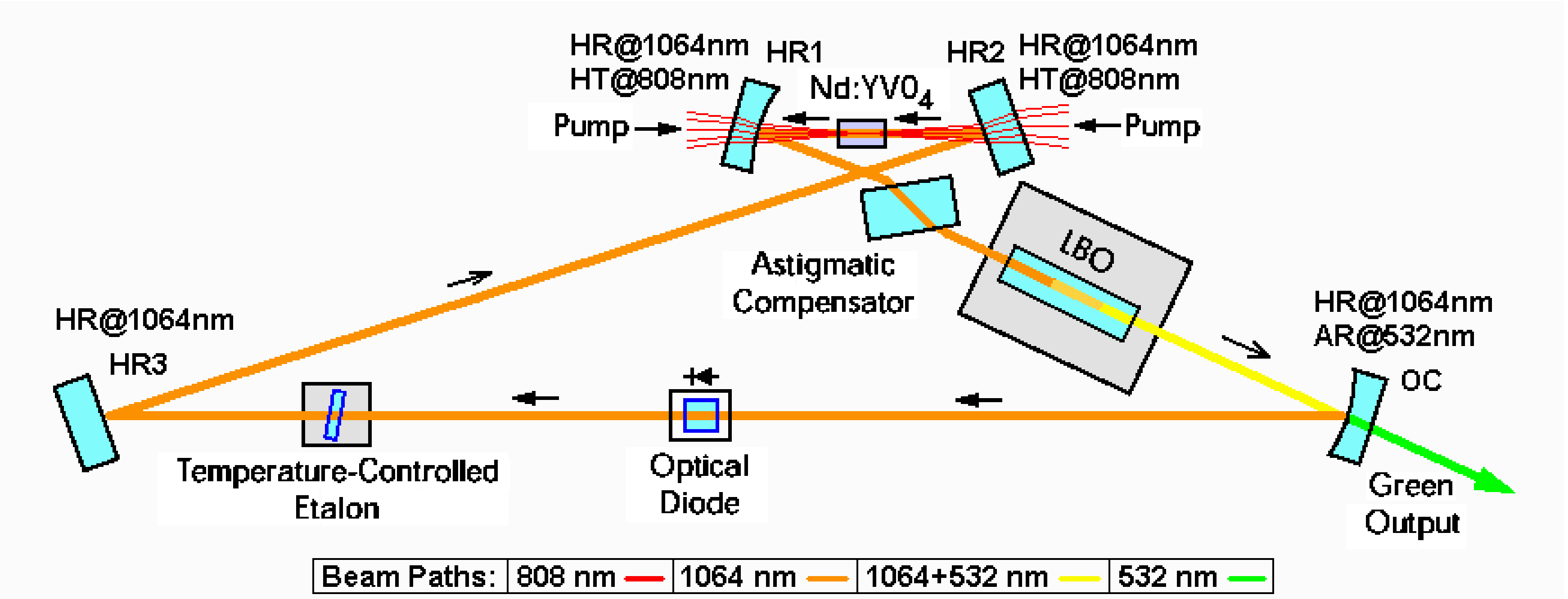

Ring Cavity Resonator of Coherent, Inc. Verdi Green DPSS Laser

www.coherent.com

Optical Sources used in the NPL Ultraviolet and Infrared DIAL System

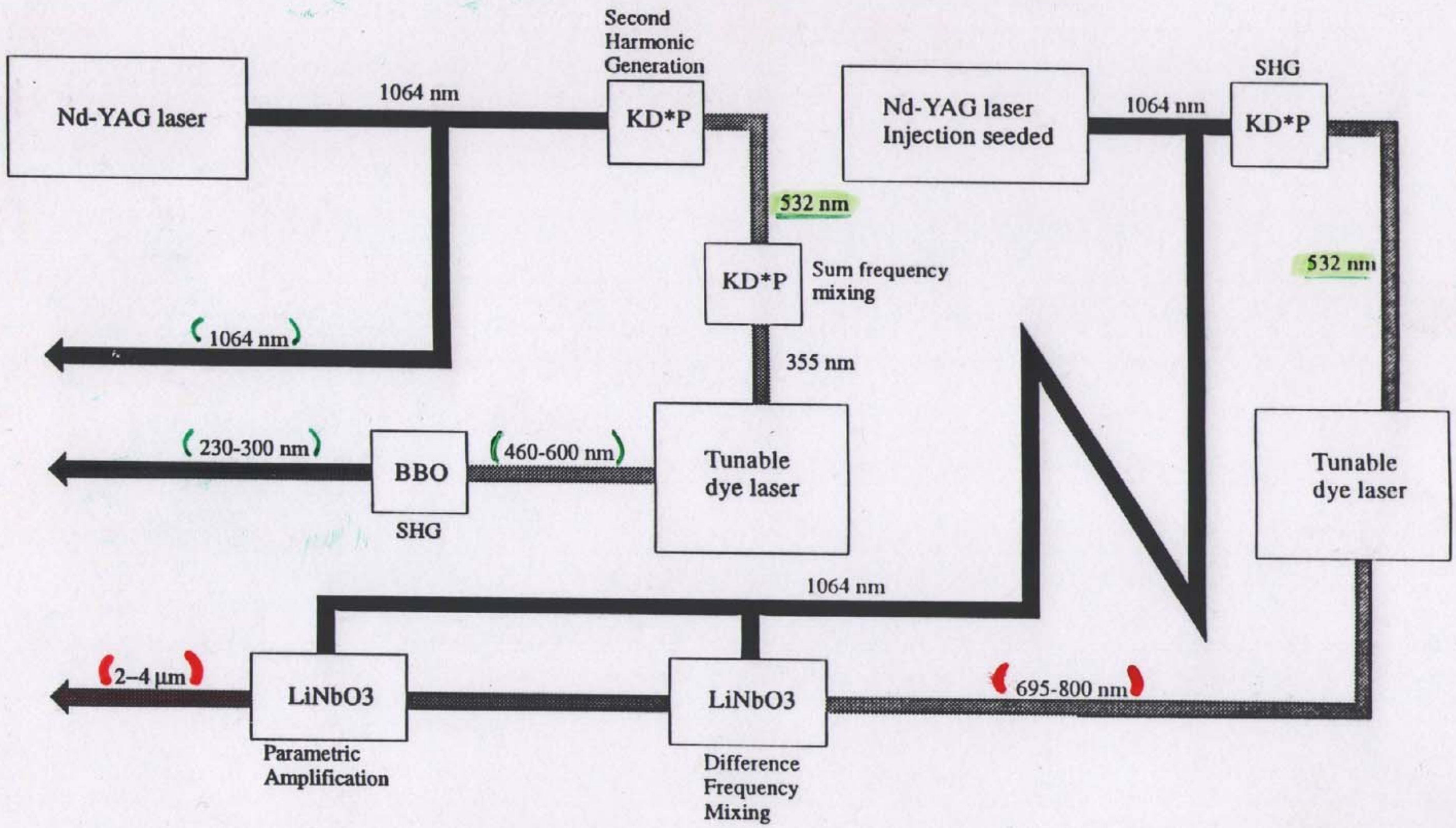

National Physical Laboratory (NPL), UK

Lidar System Components

Laser Cavity (Type II-Gas lasers-Excimer lasers):

Excited dimer

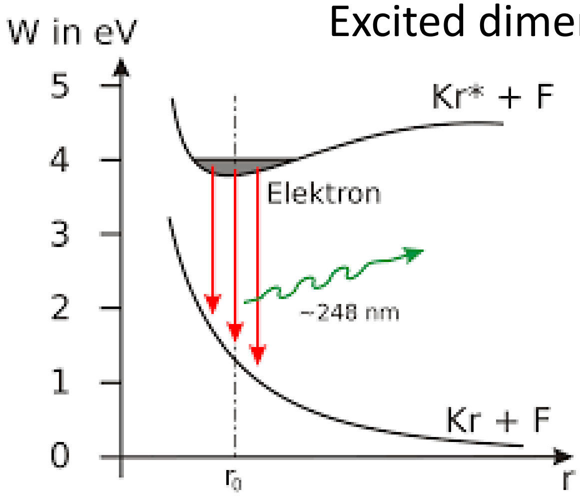

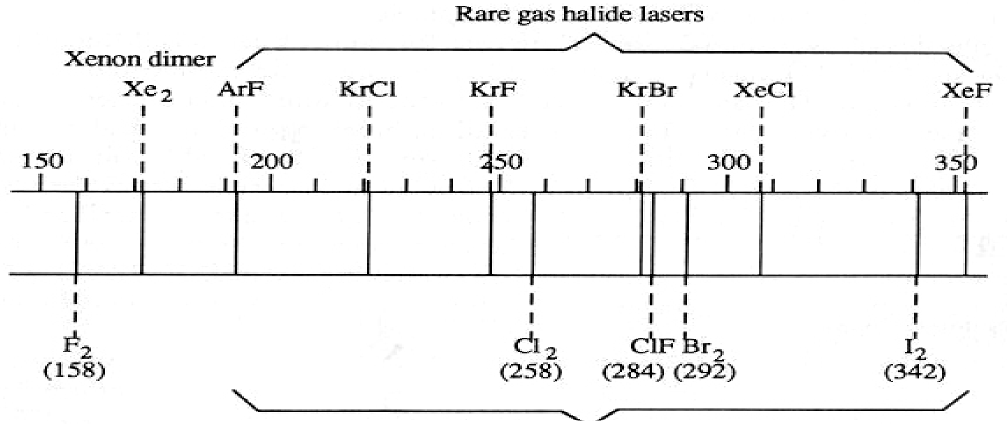

(nm)

de.wikipedia.org

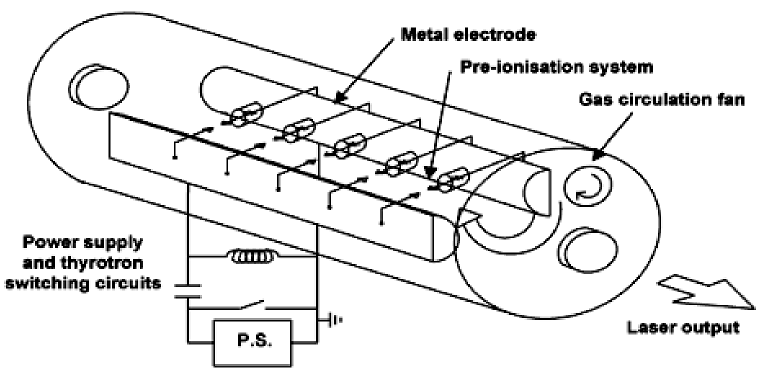

www.photonicsolutions.co.uk

Nanosecond pulses
Up to several Joules/pulse
O_3 measurements (KrF+Raman, XeCl)

http://www.twi-global.com/technical-knowledge/faqs/process-faqs/faq-what-is-an-excimer-laser/

Lidar System Components

Laser Cavity (Type III-Femtosecond lasers):

Mode-locked lasers

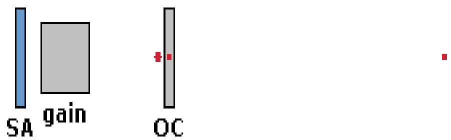

Output laser beam

SA: Saturable absorber mirror
Gain medium
OC: output coupler

Mode locking: The laser resonator contains either an **active** element (an **optical modulator**) or a nonlinear **passive** element (a **saturable absorber**), which causes the formation of an ultrashort pulse circulating in the laser resonator.

Passive mode-locking: The gain medium compensates for losses, and the saturable absorber mirror (SA) enforces pulse generation. Each time the circulating pulse hits the output coupler mirror (OC), a pulse is emitted in the output.

SA with very low losses at high energies!

www.rp-photonics.com

Femtosecond pulses
Up to several mJ/pulse

Lidar System Components

Laser Sources:

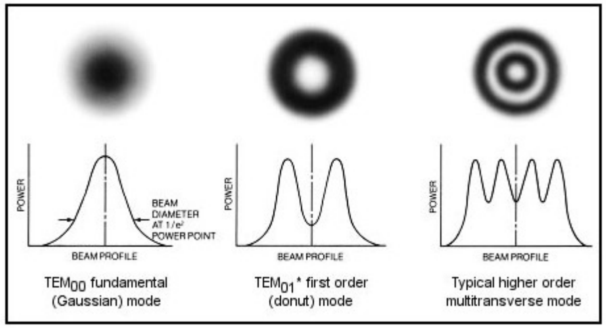

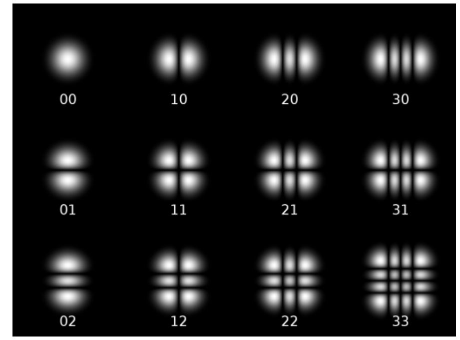

Transverse laser oscillating modes
(inside the laser cavity)

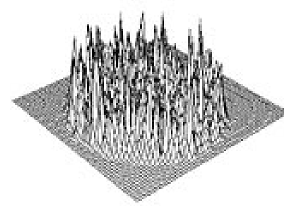

a) Multi-mode laser beams

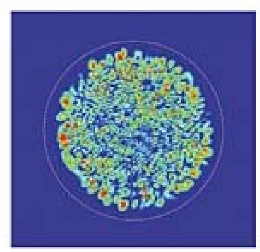

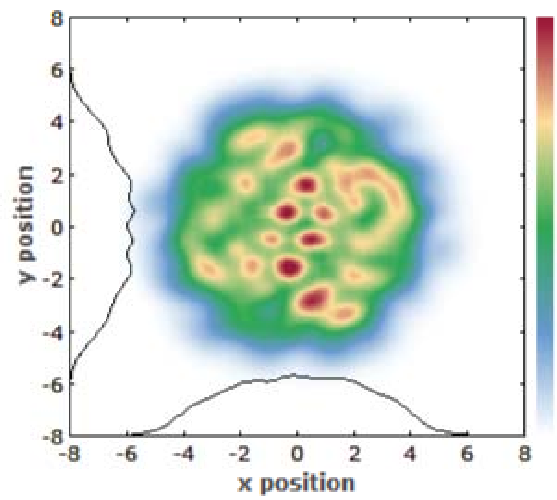

https://www.rp-photonics.com/beam_profilers.html
www.spie.org

The laser energy is distributed over several oscillating "modes", within the laser cavity

Applications:
- Detection of aerosols, molecules, clouds, etc.

Lidar System Components

Laser Sources:

b) Mono/Single-mode (single frequency): Injection seeded lasers

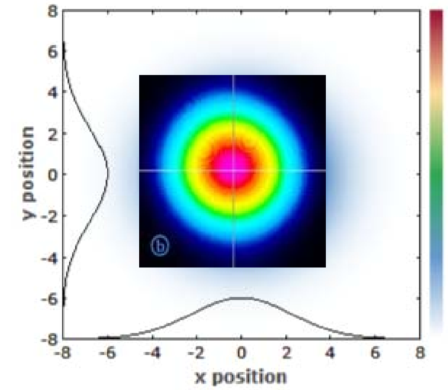

Evangellatos et al. (2013; 2014)

The laser energy is distributed over one single several oscillating "mode", within the laser cavity

Specs/Requirements:

-Very narrow laser linewidth (<1 MHz)

[@1.54 um → 1.3 MHz Doppler shift ⟷ 1 m/s wind velocity]

Applications:

- Coherent transmitter in pulsed **Doppler** lidars (measurement of wind velocity + shear)
- High Spectral Resolution Lidars-**HSRL** (aerosol backscatter-extinction, wind velocity + shear)
- Temperature profiling, etc.

Lidar System Components

Common problems related to Laser Sources:

a) Beam power instability (e.g. 266 nm)

Performance Specifications

Wavelength	Pulse Width[5]	Short Term Energy Stability[6]	Long Term Power Drift[7]
1064 nm	8–12 ns	±2%	<3%
532 nm	1–2 ns <1064 nm	±3%	<5%
355 nm	2–3 ns <1064 nm	±4%	<6%
266 nm	3–4 ns <1064 nm	±8%	<10%

6. Pulse-to-pulse stability for >99% of pulses, measured over a 1 hour period.
7. Over 8 hour period with temperature variations of <±3°C.

Source: Quanta Ray lasers (Spectra Physics)

b) Earth problems (a good earthing is required)

c) Stable input voltage is required

Laser Safety !

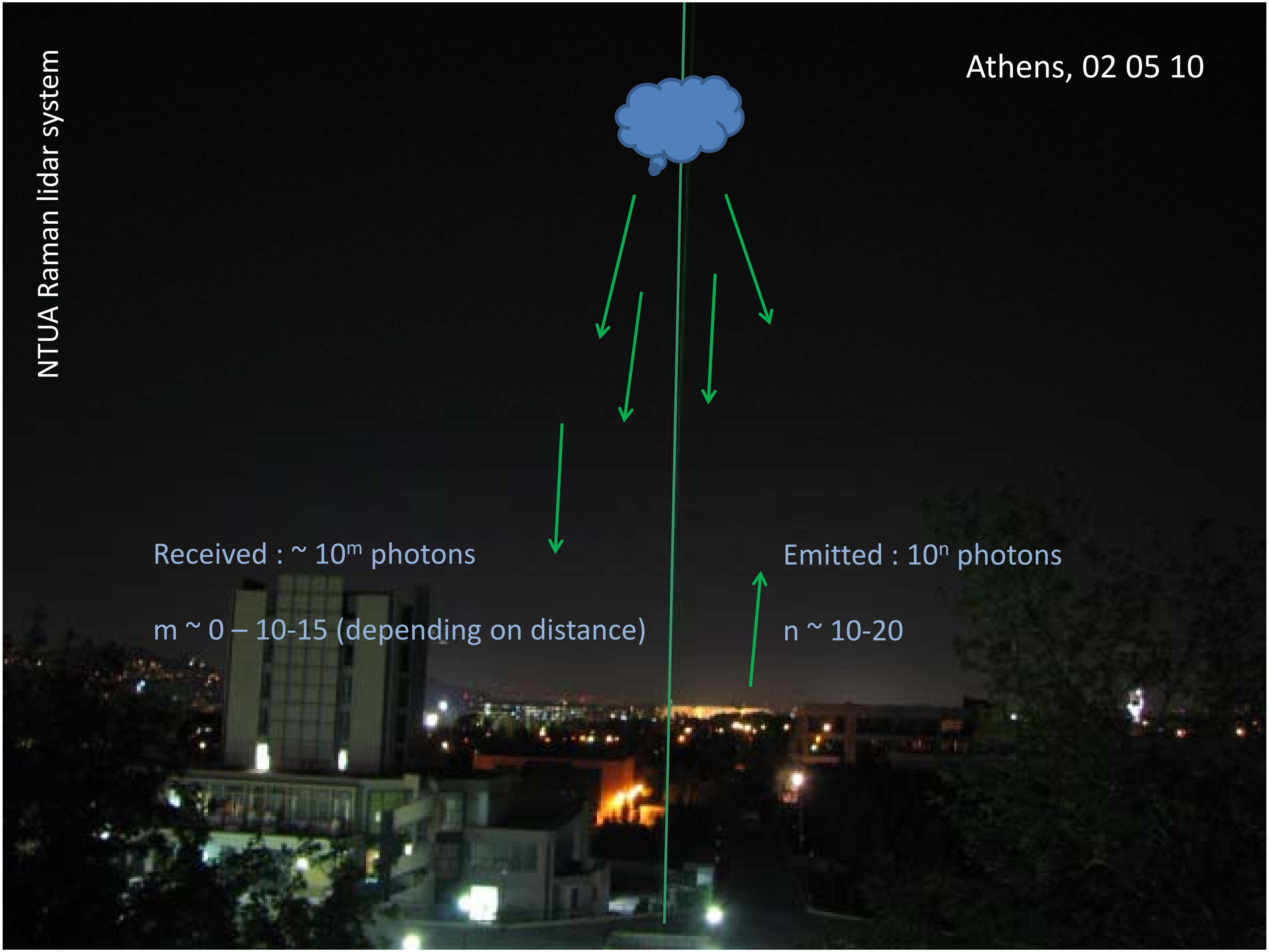
NTUA Raman lidar system
Athens, 02 05 10
Received : ~ 10m photons
m ~ 0 – 10-15 (depending on distance)
Emitted : 10n photons
n ~ 10-20

Lidar System Components

Photo-detectors (I)

PhotoMultiplier Tubes (PMTs)

Spectral Range: 110 nm – 1200 nm [lidars: 247 up to ~880 nm]
www.hamamatsu.com

Pros: Very good conversion efficiency
Cons: Only in the UV-VIS-beginning of NIR region

Photo-detectors (II)

Avalanche PhotoDiodes (APDs)

Spectral Range:
APD-Si: 200 nm – 1100 nm
APD-Ge: 800-1550 nm
APD-InGaAs [lidars: 900-1500 nm]

Pros: Good conversion efficiency
Cons: Bulky, only in the near IR

www.hamamatsu.com, www.licel.com

Lidar System Components

Photo-detectors (I)

PhotoMultiplier Tubes (PMTs) – Operating Principle

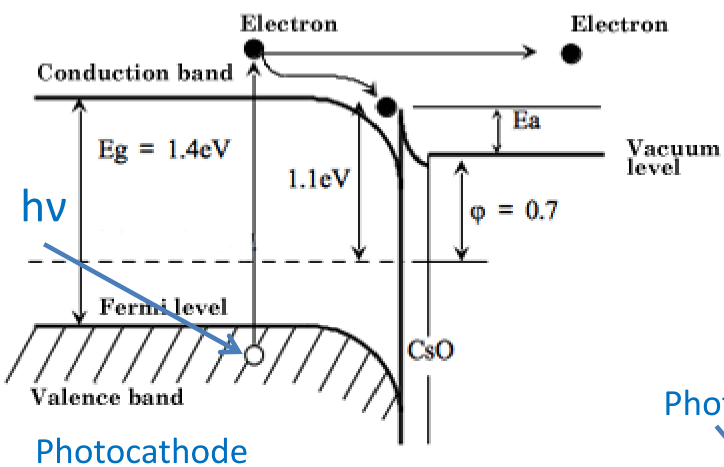

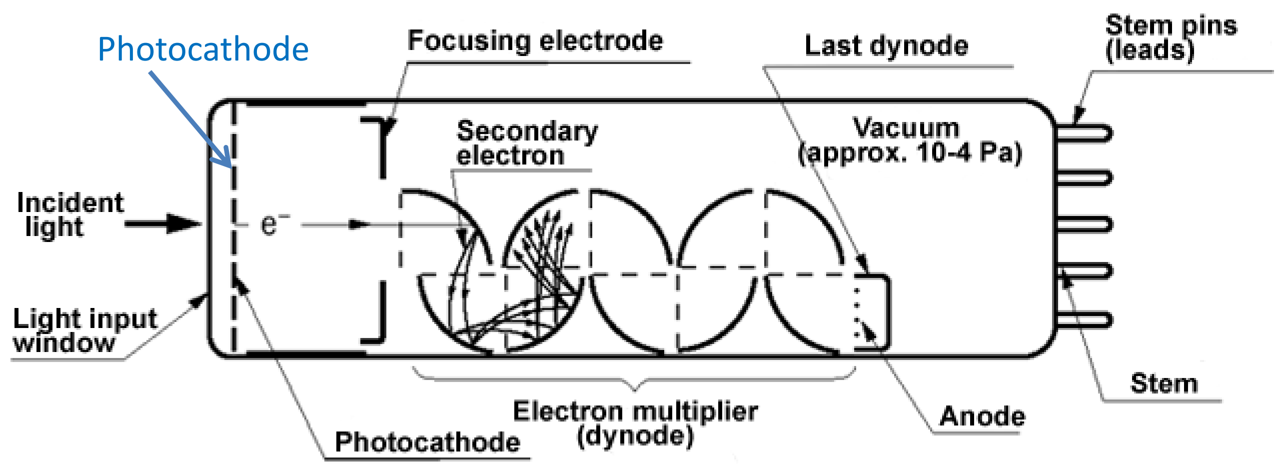

www.hamamatsu.com

Lidar System Components

Photo-detectors (I)

PhotoMultiplier Tubes (PMTs) - Operating Principle for detecting pulsed (lidar) signals

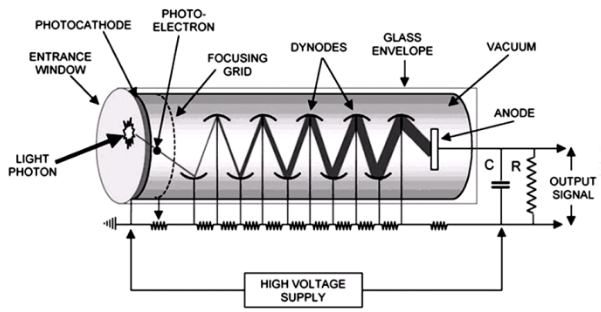

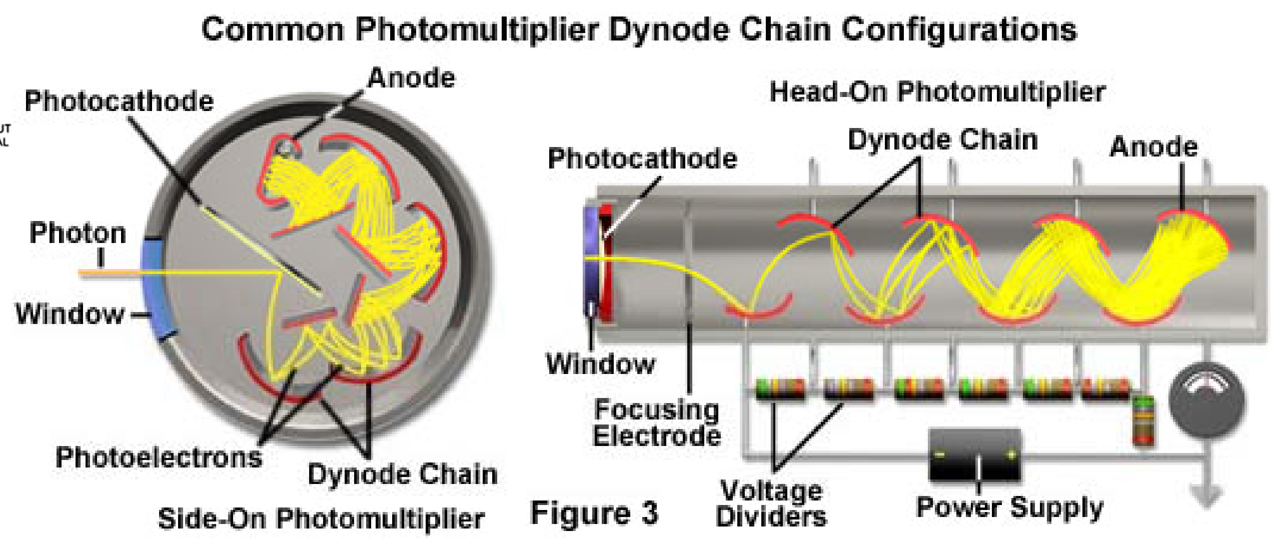

Side-on

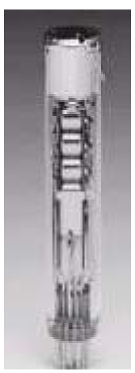

Head-on

www.olympusmicro.com

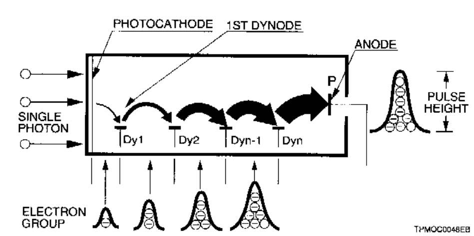

High voltage divider circuit: divide the high voltage (800-1000 V) to the dynodes

Lidar System Components

Photo-detectors (I)

PhotoMultiplier Tubes (PMTs) - Housing

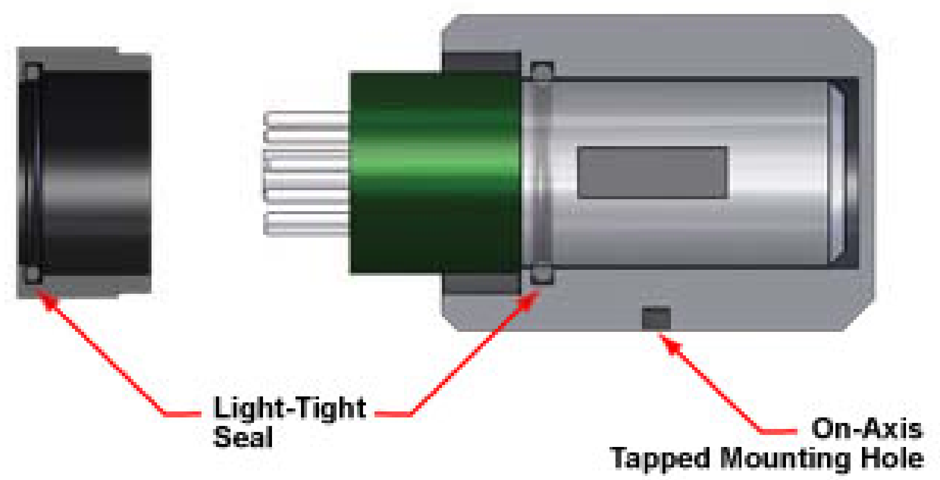

www.thorlabs.com

A proper metallic housing (magnetic shielding) is required to protect the very sensitive PMT from :

- external EM fields
- ambient temperature
- humidity

Lidar System Components

Photo-detectors (I)

PhotoMultiplier Tubes (PMTs) – Photocathode materials

The response of a PMT is specified by the **photocathode sensitivity**:

- **Quantum efficiency (%):**

QE = Nphotoel. emitted by the photocathode/Number incident photons

- **Cathode radiant sensitivity (mA/W):**

Photocurrent produced (mA) in response to the incident light power (W)
QE(%)=[124/λ(nm)] * radiant sensitivity (mA/W)

- **Cathode luminous sensitivity (µA/lm):**

It relates the photocathode current to the human eye response

Current produced by an incident flux of 1 lumen from a Tungsten filament source (@2856 K)

Lidar System Components

Photo-detectors (I)

PhotoMultiplier Tubes (PMTs) – Photocathode materials

The response of a PMT is specified by the photocathode sensitivity

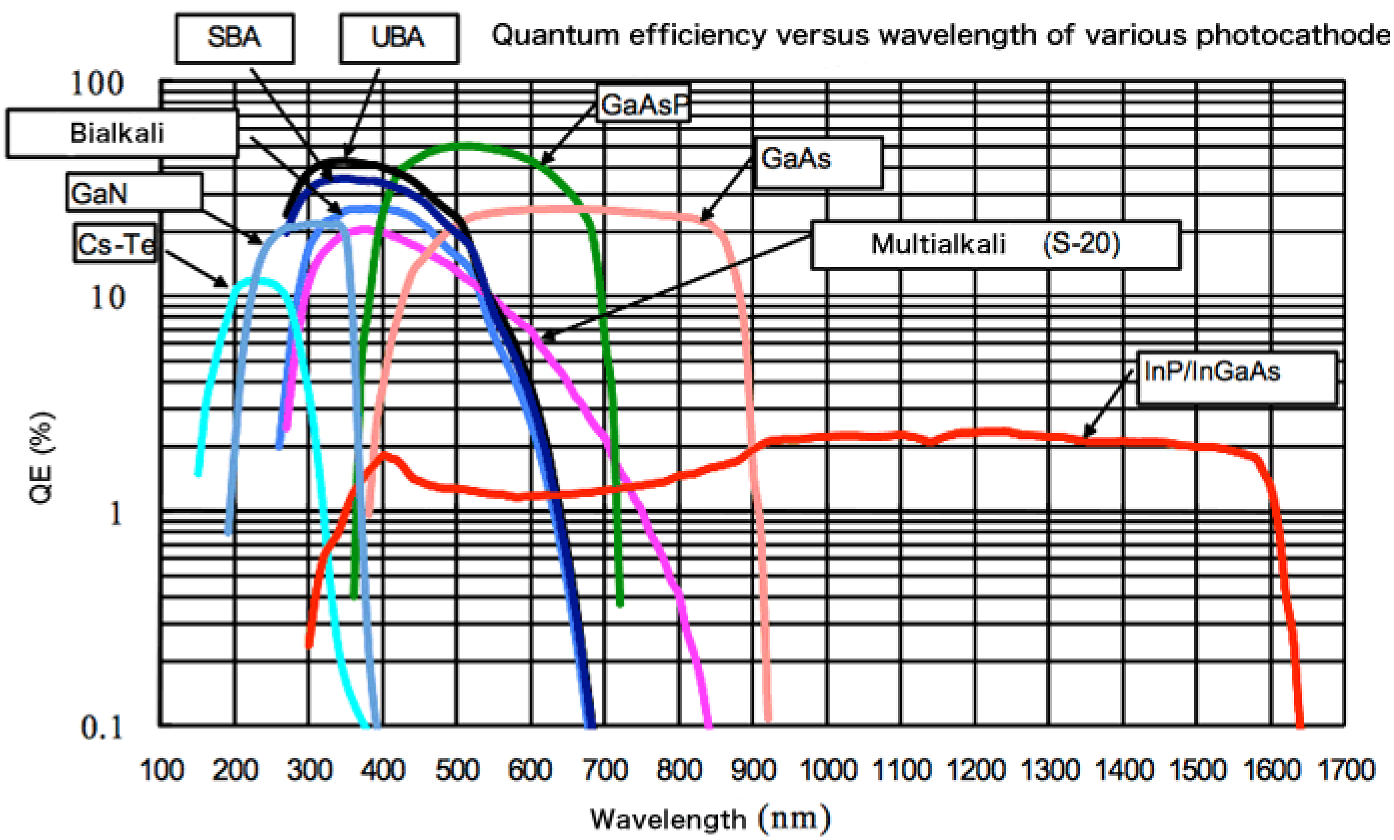

www.hamamatsu.com

Lidar System Components

Photo-detectors (I)

PhotoMultiplier Tubes (PMTs) - Photocathode

Figure 4. Spectral response curves of alkali metal type photocathode on left and crystal type c
right. ①Multialkali. ②Extended Multialkali, ③Bialkali
④Cs-Te, ⑤GaAs, ⑥Extended GaAsP, ⑦GaAsP

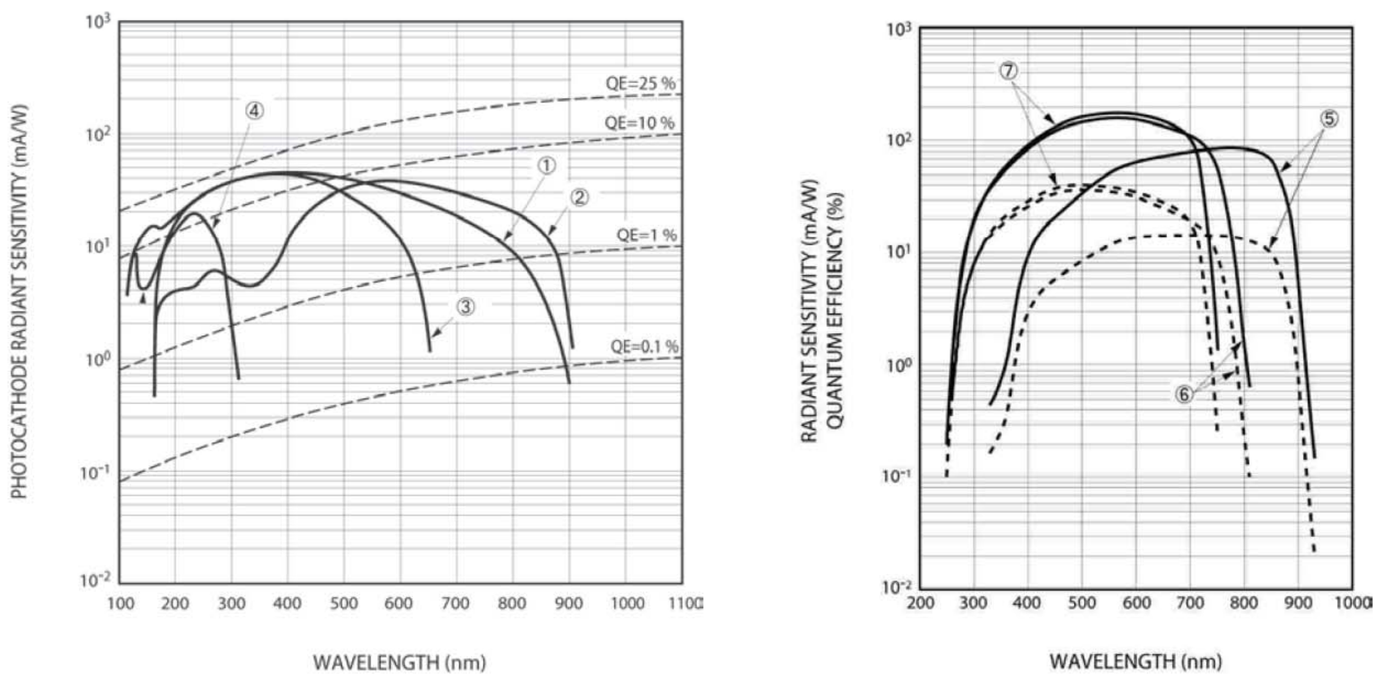

Photo-detectors (I)

PhotoMultiplier Tubes (PMTs) - Photocathode

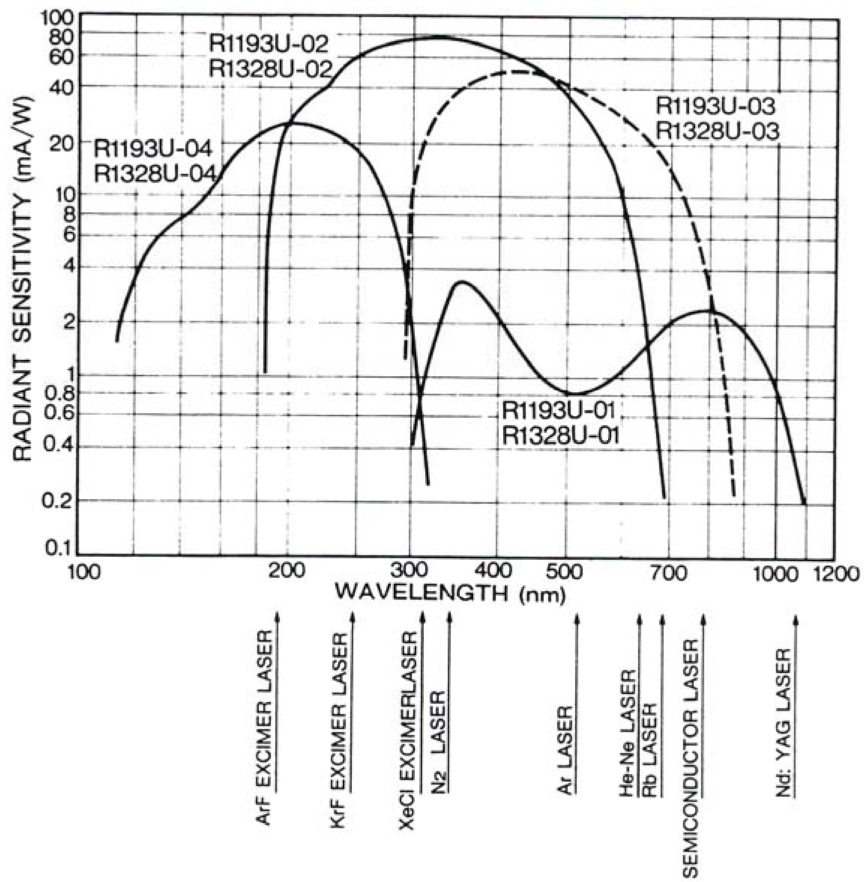

www.hamamatsu.com

Lidar System Components

Photo-detectors (I)

PhotoMultiplier Tubes (PMTs) - Photocathode

Spectral response: 1 photon (W) → anode (mA)

Gain: 1 photon → Nr photo-electrons (e^-)

■ SPECTRAL RESPONSE

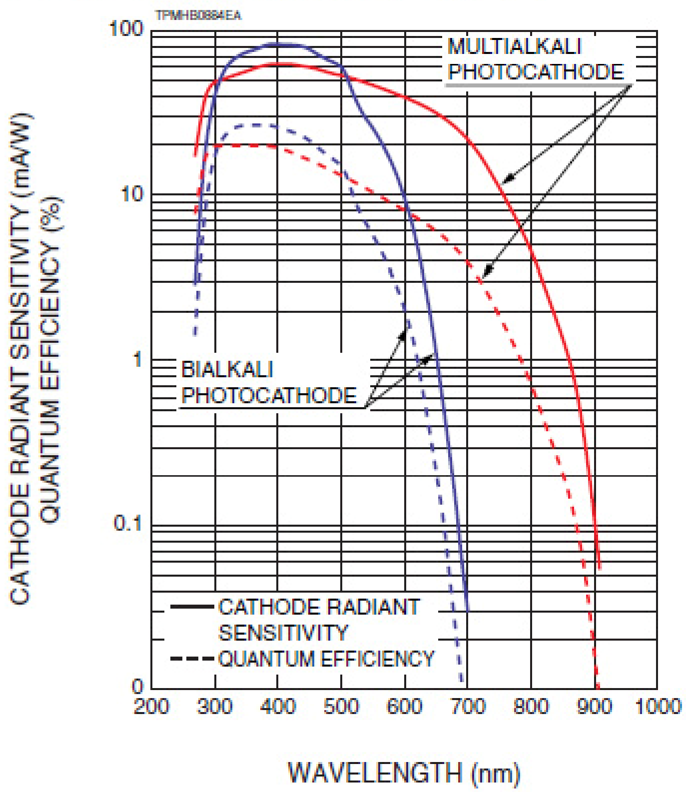

■ GAIN

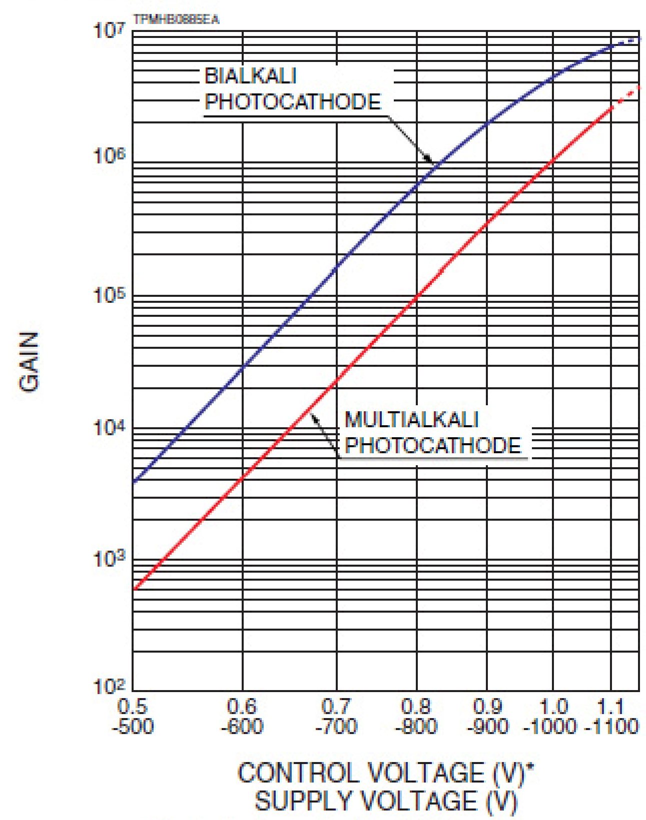

* Control voltage of a Micro PMT module.

www.hamamatsu.com

Lidar System Components

Photo-detectors (I)

PhotoMultiplier Tubes (PMTs) – Spatial uniformity

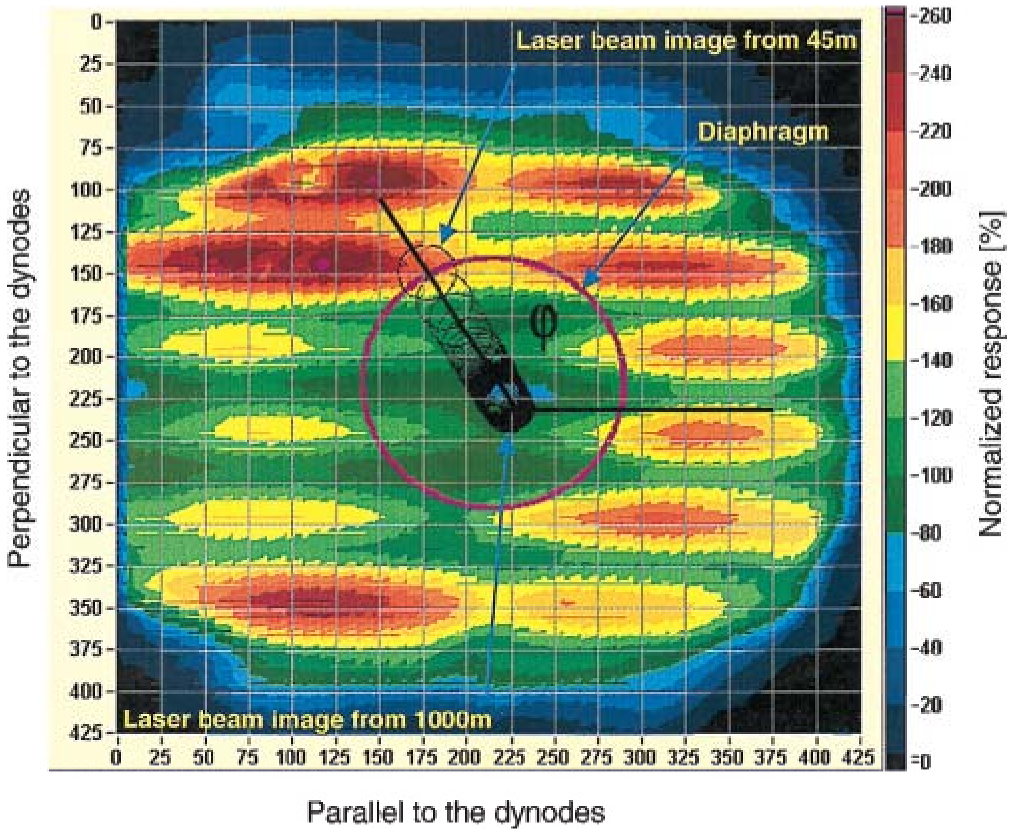

Hint: Always use doublet lenses in front of the PMTs
to direct the light into a diam ~ 3mm

Simeonov, et al., 1999.

Lidar System Components

Photo-detectors (I)

PhotoMultiplier Tubes (PMTs) – Spatial uniformity

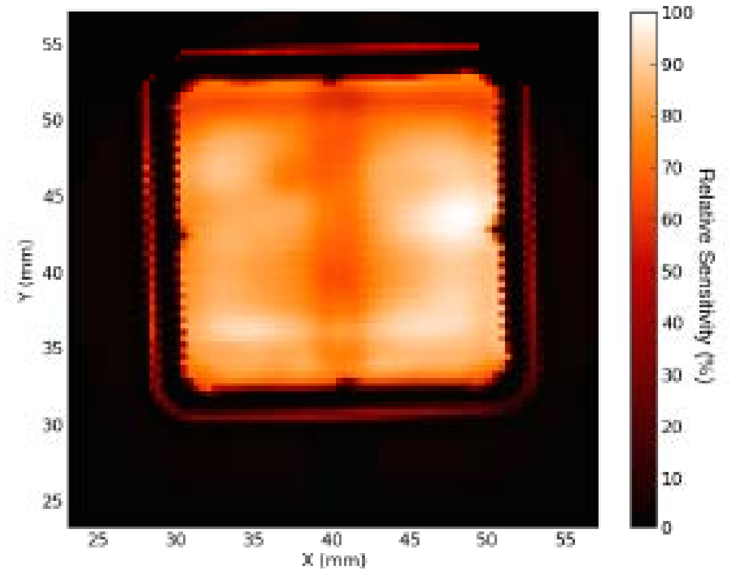

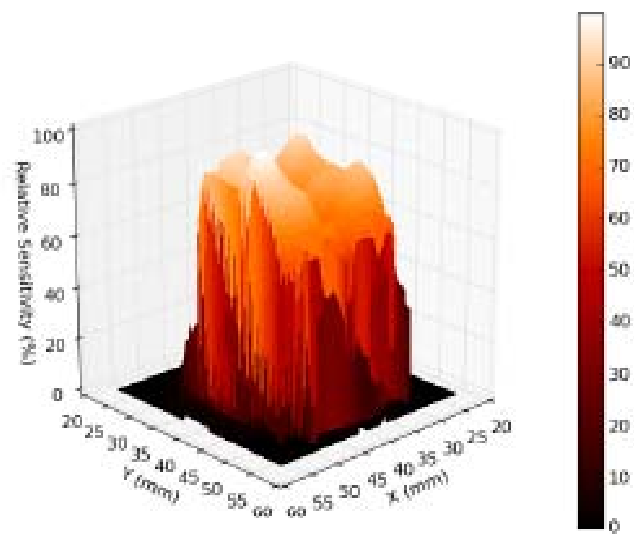

Lidar System Components

Photo-detectors (I)

PhotoMultiplier Tubes (PMTs) – Anode collection space

The anode collection should have a suitable geometry for:

- collecting all secondary electrons emitted by the last dynode

- minimizing space charge effects to ensure linear response in pulse-mode operation

- matching the anode impedance to the characteristic impedance of the output connection (e.g, signal digitizer).

Anode sensitivity = Cathode sensitivity * PMT Gain

www.hamamatsu.com

Lidar System Components

Photo-detectors (I)

PhotoMultiplier Tubes (PMTs) – Problems

- Never exceed the maximum average DC anode current (< 100 μA, or 5mV @50Ω input → Atmospheric background !)
- Never exceed the maximum voltage ratings
- After pulses (spurious pulses at low signal levels):

Main causes:

-**Luminous reactions** (light emitted by the electrodes due to electron bombardment by high level light pulses)
- Ionization of residual traces gases
- PMT lifetime ~ 1/number of incident photons (N_{ip})
- Change your PMT when its lifetime is exceeded !
- Linearity – Non linearity (Nr of electrons collected ~ Nr of incident pulses)

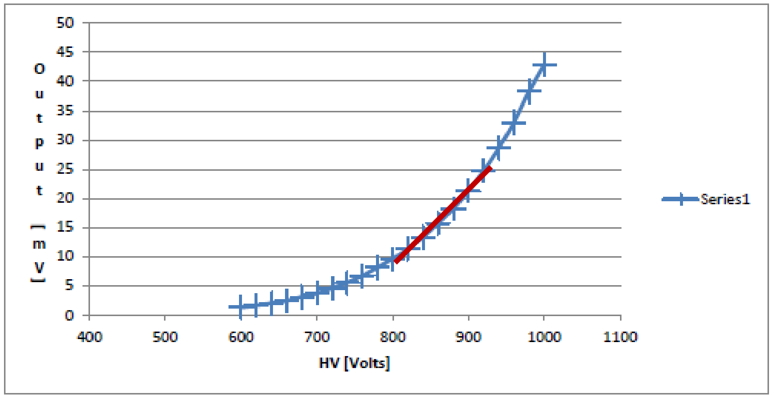

PMT Linear region (output vs HV, with const. light level input)

Kokkalis, PhD Thesis (2014)

Photo-detectors (I)

PhotoMultiplier Tubes (PMTs) – Photon Counting mode

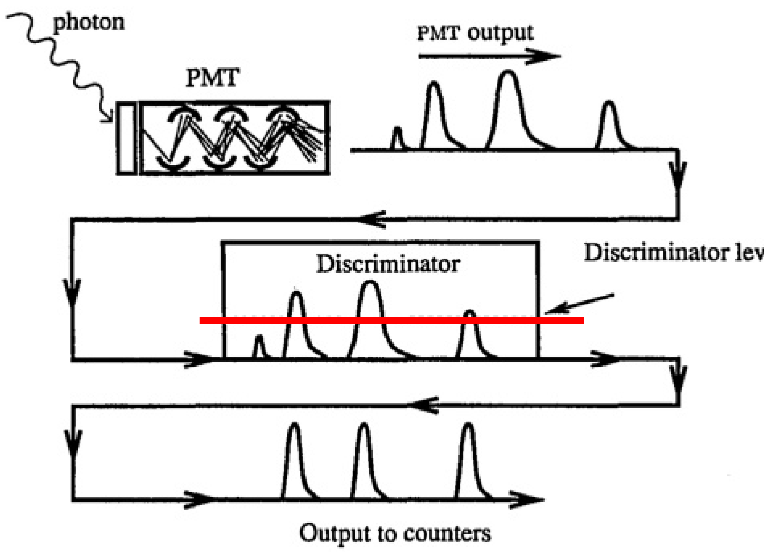

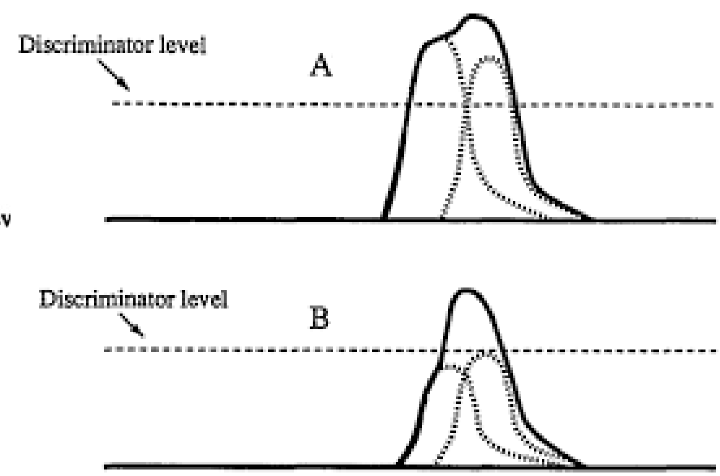

Pulse pileup effect

A: Count loss from pulse pileup

B: Count gain from pulse pileup

Donovan et al. (1993)

Lidar System Components

Photo-detectors (I)

PhotoMultiplier Tubes (PMTs) – Photon Counting mode

Photon counting regime:

Low light level: PMT responses **linearly** (the output signal is proportional to the incident light intensity),

High light level: PMT responses **NON-linearly** (the output signal is NOT proportional to the Incident light intensity) → overlapping of light pulses (pulse pileup effect)

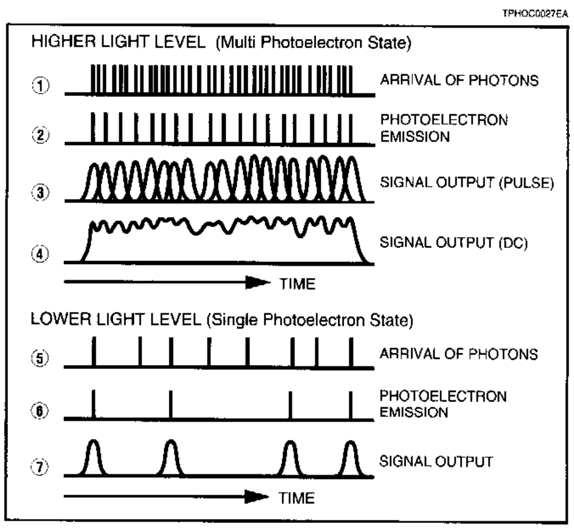

High light level

Low light level

www.hamamatsu.com

Lidar System Components

Photo-detectors (II)

Avalanch PhotoDiodes (APDs)

1) Incident photons are **absorbed**

2) Electrons and holes are produced (p^- region)

3) Electrons are accelerated (in the absorption region), thanks to E(x), collide with valence e^- and, thus, produce free electrons (p region)

4) Electrons are accelerated, in the avalanche region, thanks to E(x) [100 kV/cm) , and produce secondary e^- (depleted region) through impact ionization.

Reverse bias electric field

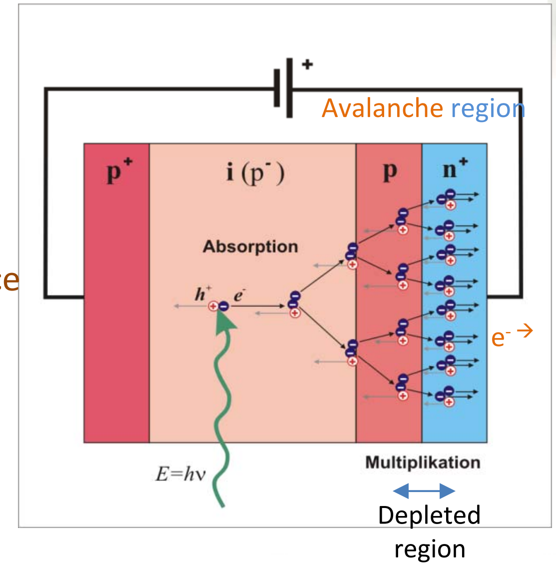

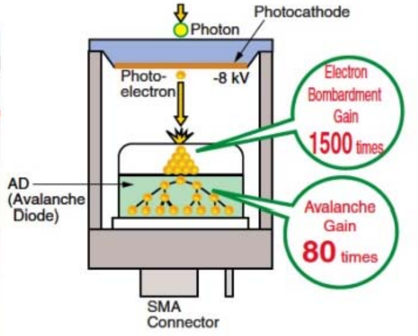

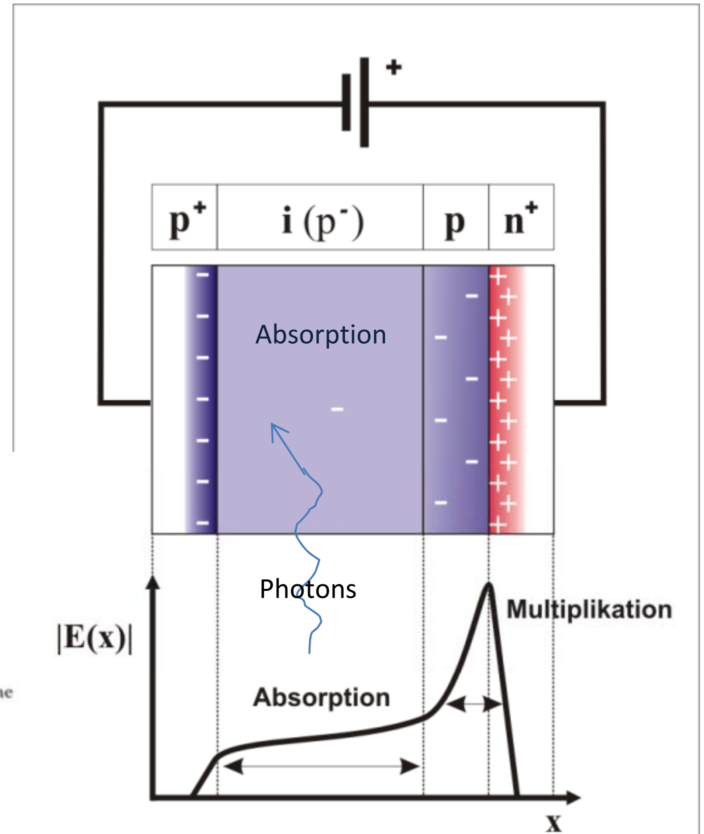

www.wikiwand.com/de/Avalanche-Photodiode

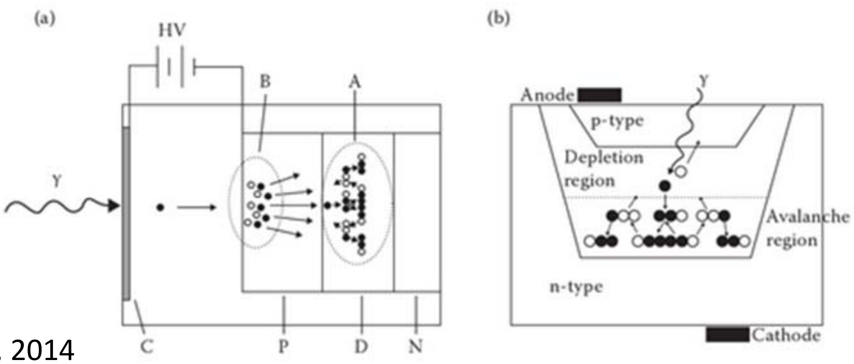

Marcu et al., 2014

Photo-detectors (II)

Avalanch PhotoDiodes (APDs)

Spectral response: 1 photon (W) → anode (A)

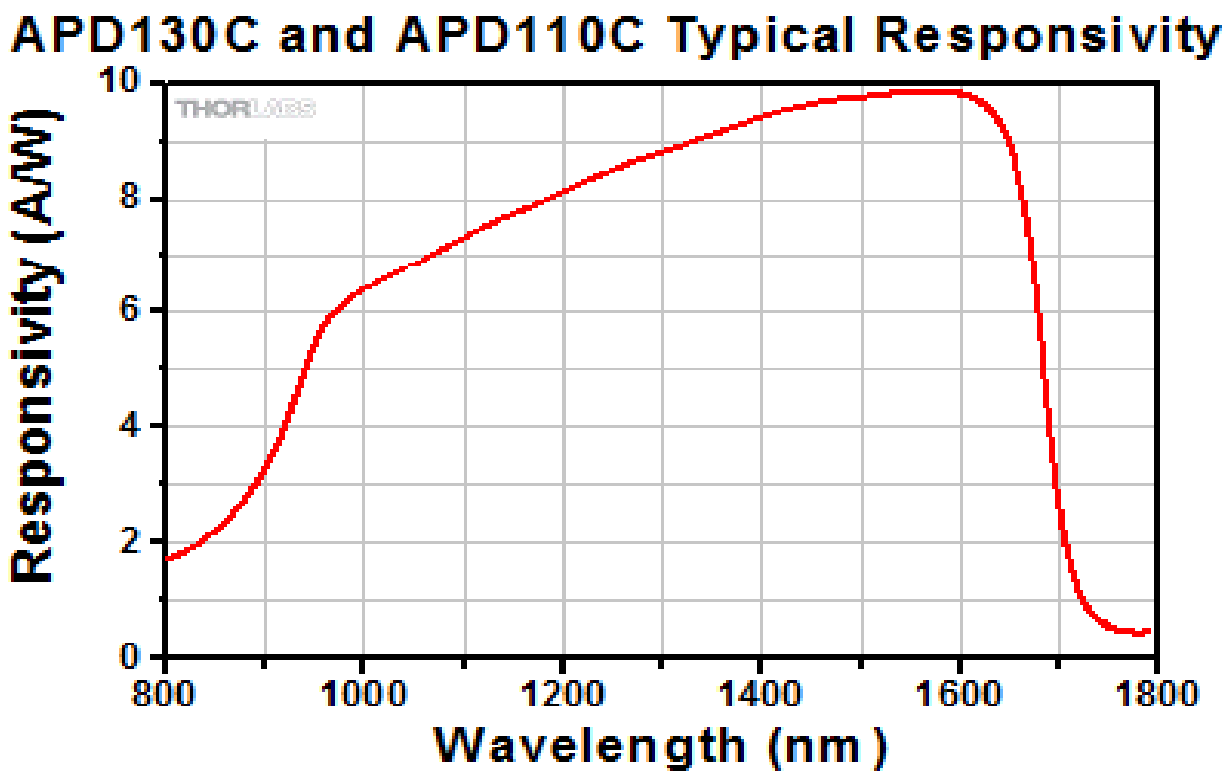

www.hamamatsu.com

Lidar System Components

Photo-detectors (I-II)

PMTs - APDs– Anode dark current

Anode dark current (in total darkness the PMT still produces a small output current)

- Ohmic leakage currents (leakage currents between electrodes and the glass)
- Thermionic current (thermionic emission of electrons from the photocathode)

NTUA, EOLE data

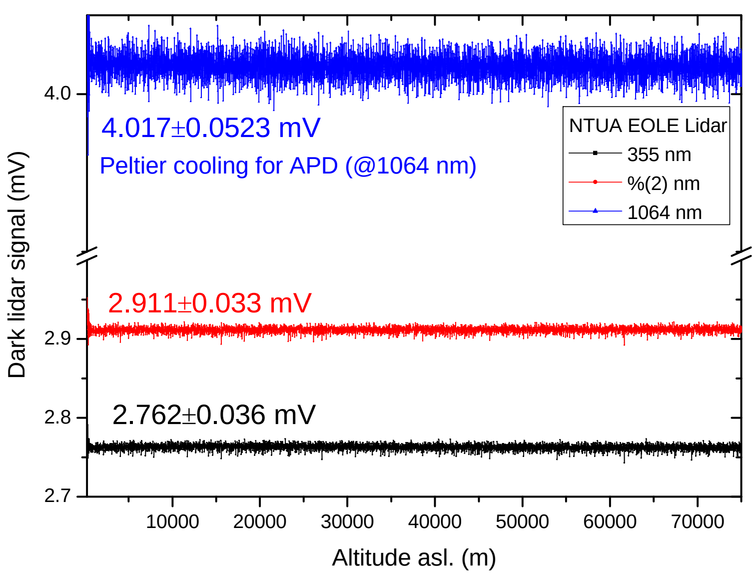

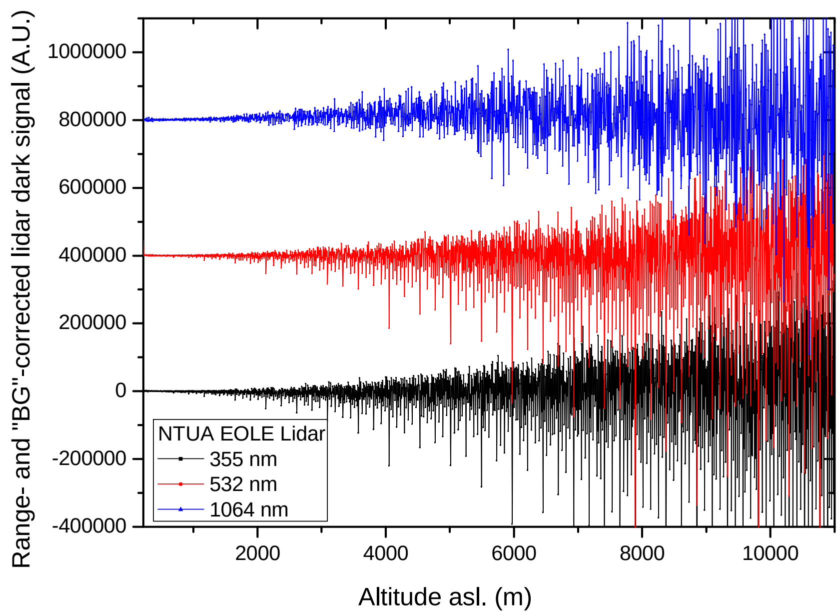

Signal Detection

Lidar Signal

Analog mode

Photon counting mode

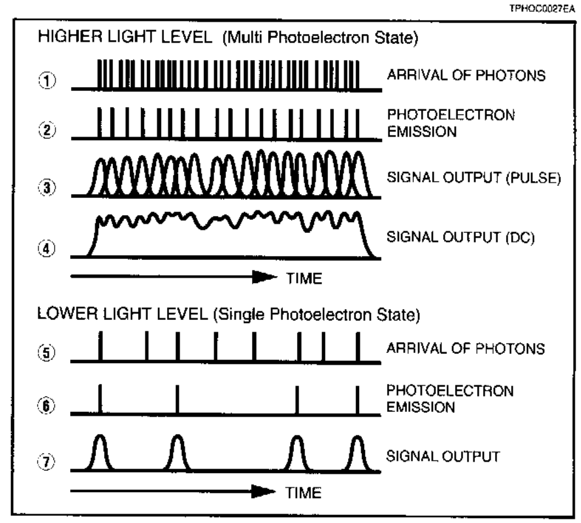

www.hamamatsu.com

Lidar Signal

PMT output

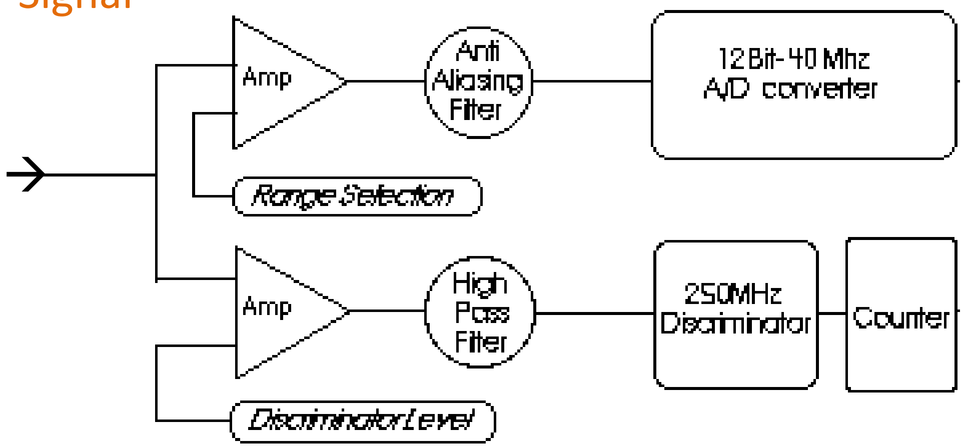

Analog mode

Photon counting mode

www.licel.com

Analog to Digital Conversion (12-, 14-, 16-bit Digitizers)

Signal ADC & Digitization/Sampling (Analog signals)

$\Delta t^*=1/F_D$, F_D=Signal sampling frequency (10-40 MHz → ~ GHz)

Example:

F_D=10 MHz → Δt^*=100 ns → Δz=15 m
F_D=20 MHz → Δt^*=50 ns → Δz=7.5 m
F_D=40 MHz → Δt^*=25 ns → Δz=3.75 m
F_D=1 GHz → Δt^*=1 ns → Δz=0.15 m

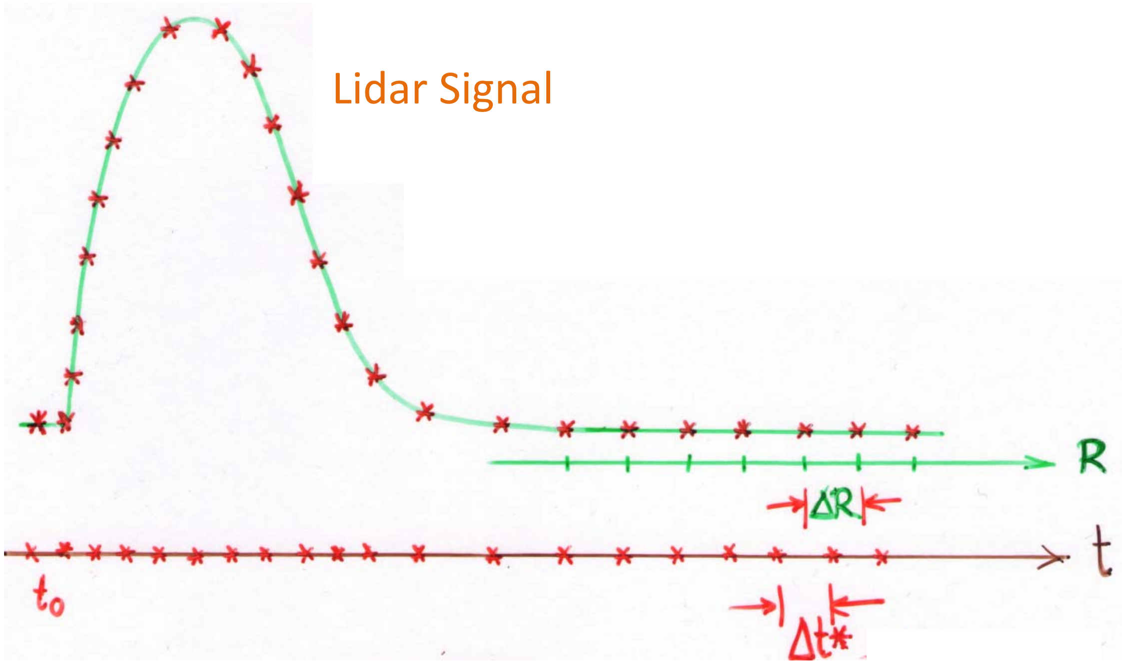

Signal ADC & Digitization/Sampling (Analog signals)

Rule of thumb: Max Analog signal/2, e.g. for 40 mV input signal → signal range 100 mV

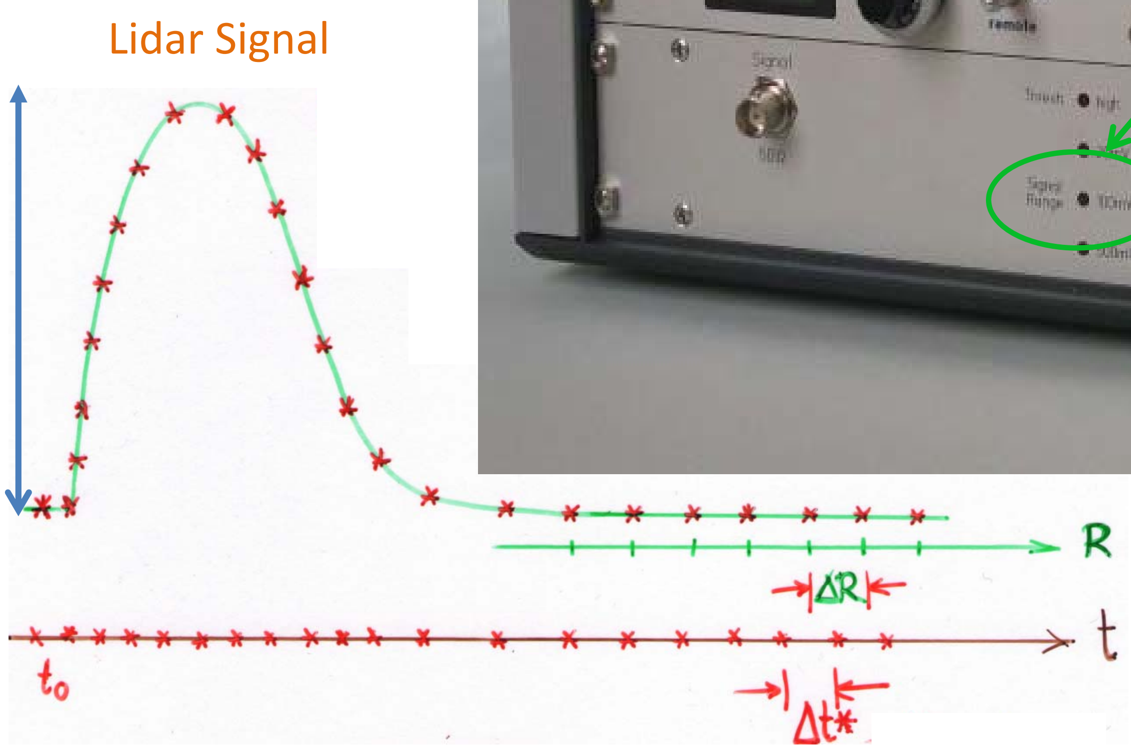

Signal (Photon Counting mode)

Lidar Signal → Photon counting mode

(Dead time correction)

3. NONPARALYZABLE SYSTEM

(1) $$N = \frac{S}{1 + S * \tau_d}$$

N - is the observed countrate
S - is the true countrate
τ_d - is the system dead time

While the paralyzable case is nonlinear equation, the nonparalyzable case can be easily inverted to

(2) $$S = \frac{N}{1 - N * \tau_d}$$

As both cases are only a theoretical model, they are valid for lower countrates but fail when $S * \tau_d$ becomes larger than one. From a numerical point of view Eq. 2 can be only applied to a signal as long as

(3) $$N < \tau_d$$

www.licel.com

For each PMT a dead time (τ_d) has to be measured !!

Example:

Alt= 0.5 km → N_{meas}=50 MHz, τ_d=3.8 ns → S_{true}=61.75 MHz

Alt= 3 km → N_{meas}=10 MHz, τ_d=3.8 ns → S_{true}=10.4 MHz

All photon counting signals (low altitudes) have to me corrected for dead time (N_{meas}>10MHz)

Signal (Photon Counting mode)

Lidar Signal → Photon counting mode (Dead time correction)

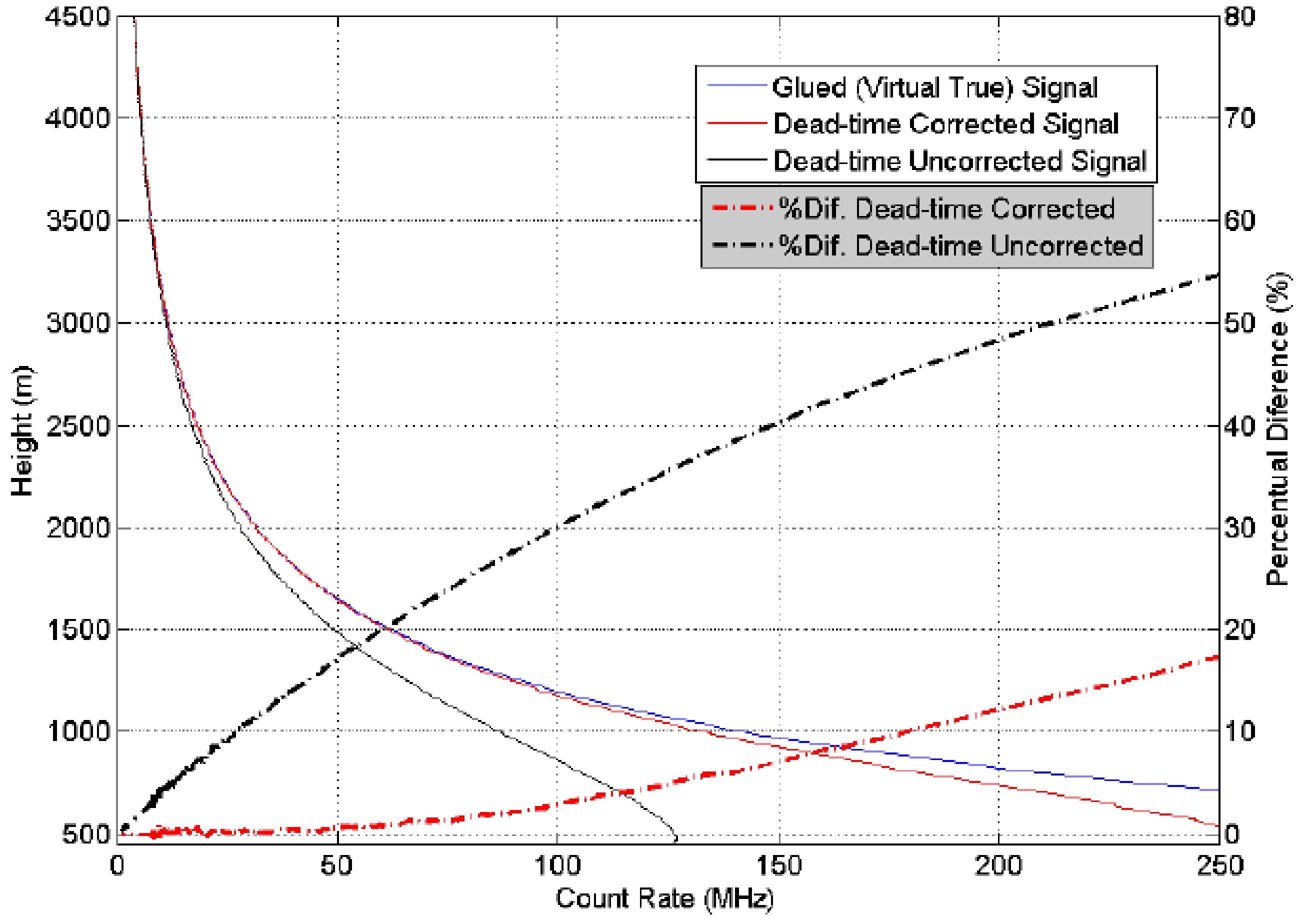

Barbosa et al., 2014

Examples (I)

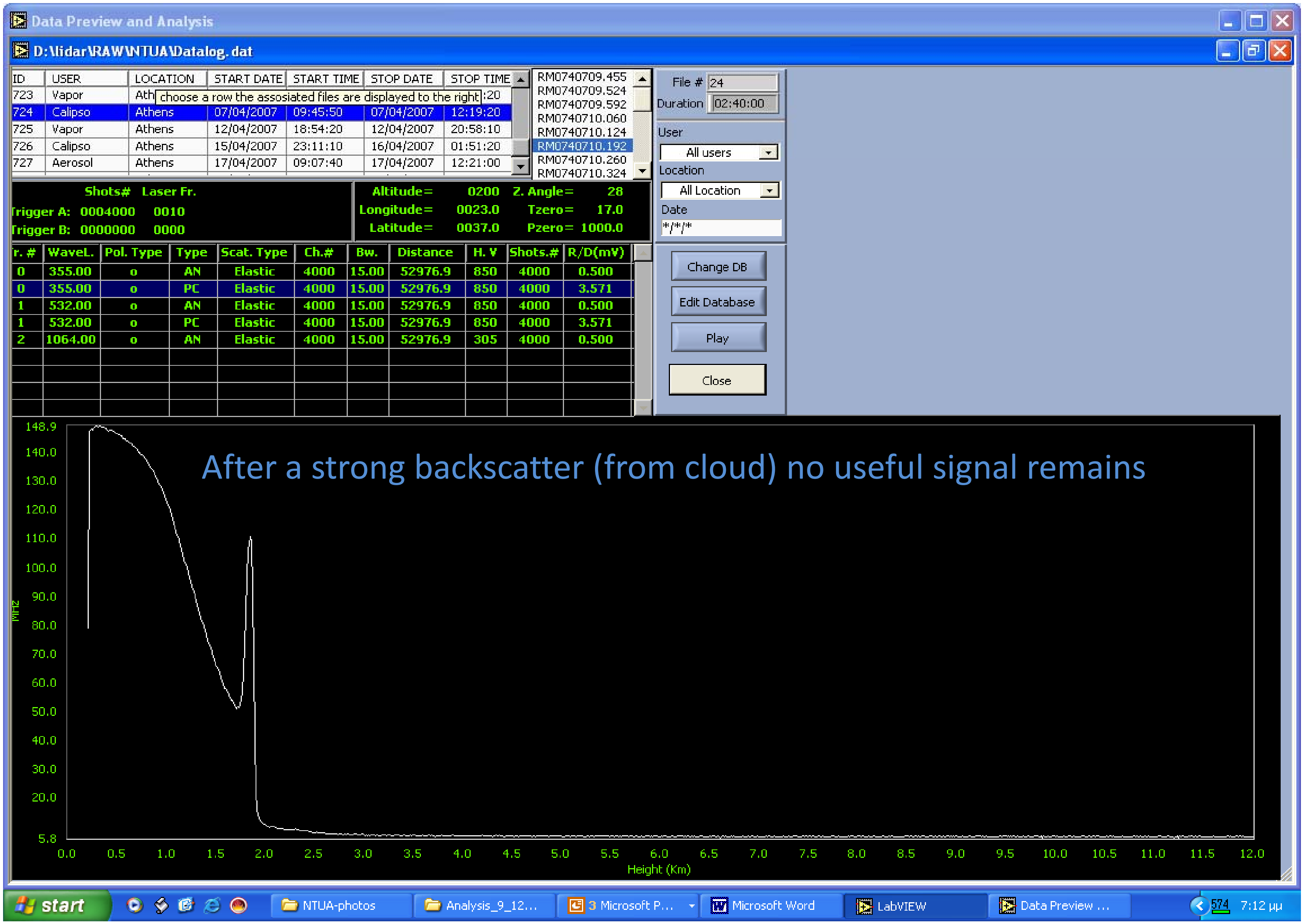
Data Preview and Analysis
D:\lidar\RAW\NTUA\Datalog.dat
ID USER LOCATION START DATE START TIME STOP DATE STOP TIME
723 Vapor Ath choose a row the assosiated files are displayed to the right
724 Calipso Athens 07/04/2007 09:45:50 07/04/2007 12:19:20
725 Vapor Athens 12/04/2007 18:54:20 12/04/2007 20:58:10
726 Calipso Athens 15/04/2007 23:11:10 16/04/2007 01:51:20
727 Aerosol Athens 17/04/2007 09:07:40 17/04/2007 12:21:00
RM0740709.455
RM0740709.524
RM0740709.592
RM0740710.060
RM0740710.124
RM0740710.192
RM0740710.260
RM0740710.324
File # 24
Duration 02:40:00
User
All users
Location
All Location
Date
Shots# Laser Fr.
Trigger A: 0004000 0010
Trigger B: 0000000 0000
Altitude= 0200 Z. Angle= 28
Longitude= 0023.0 Tzero= 17.0
Latitude= 0037.0 Pzero= 1000.0
Wavel. Pol. Type Type Scat. Type Ch.# Bw. Distance H. V Shots.# R/D(mV)
0 355.00 o AN Elastic 4000 15.00 52976.9 850 4000 0.500
0 355.00 o PC Elastic 4000 15.00 52976.9 850 4000 3.571
1 532.00 o AN Elastic 4000 15.00 52976.9 850 4000 0.500
1 532.00 o PC Elastic 4000 15.00 52976.9 850 4000 3.571
2 1064.00 o AN Elastic 4000 15.00 52976.9 305 4000 0.500
Change DB
Edit Database
Play
Close
After a strong backscatter (from cloud) no useful signal remains
Height (Km)
start
NTUA-photos
Analysis_9_12...
3 Microsoft P...
Microsoft Word
LabVIEW
Data Preview ...
7:12 μμ

Examples (II)

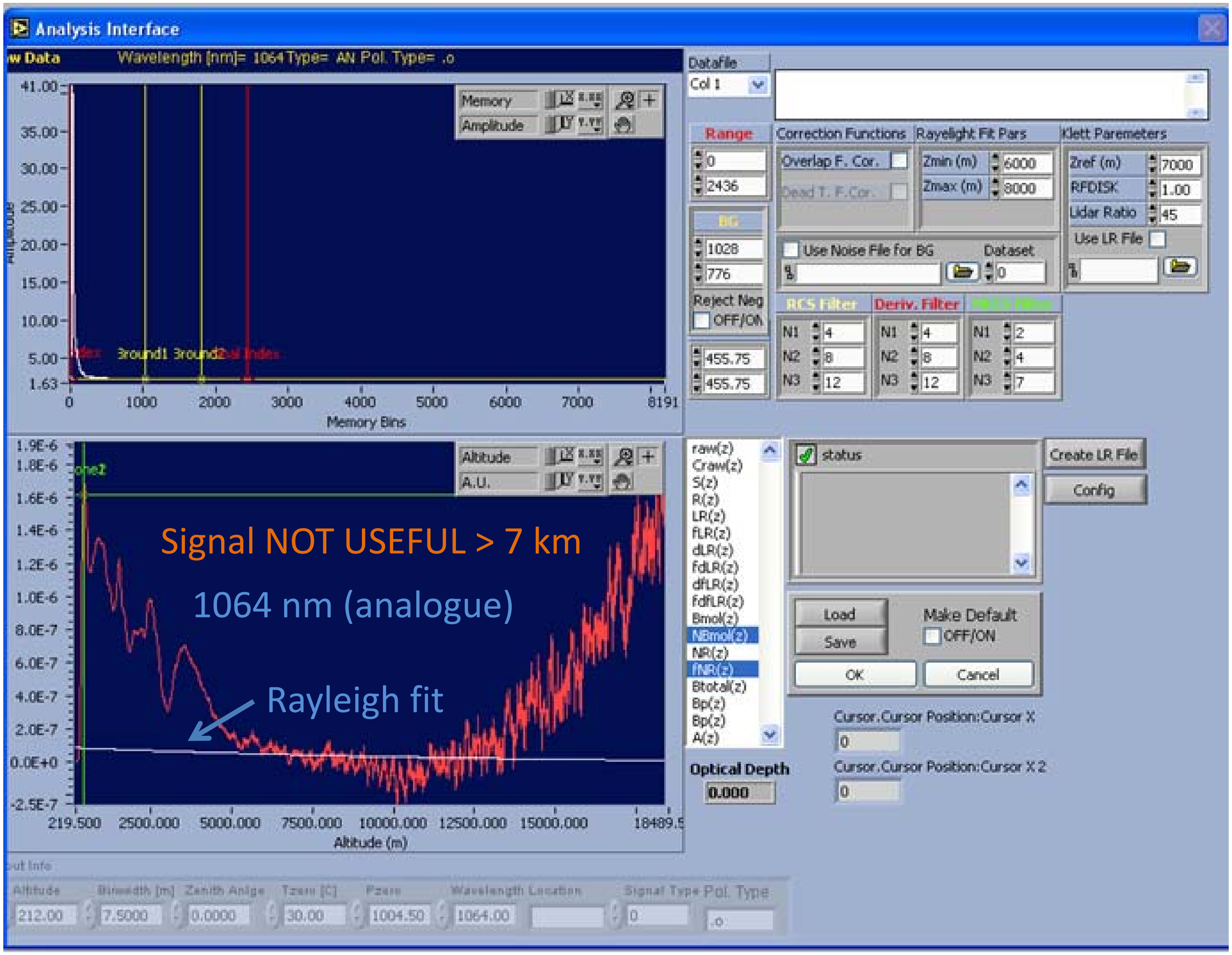

Examples (III)

PROBLEM : (not stable signal > 7 km height)

Raw lidar signal with strong dust layer

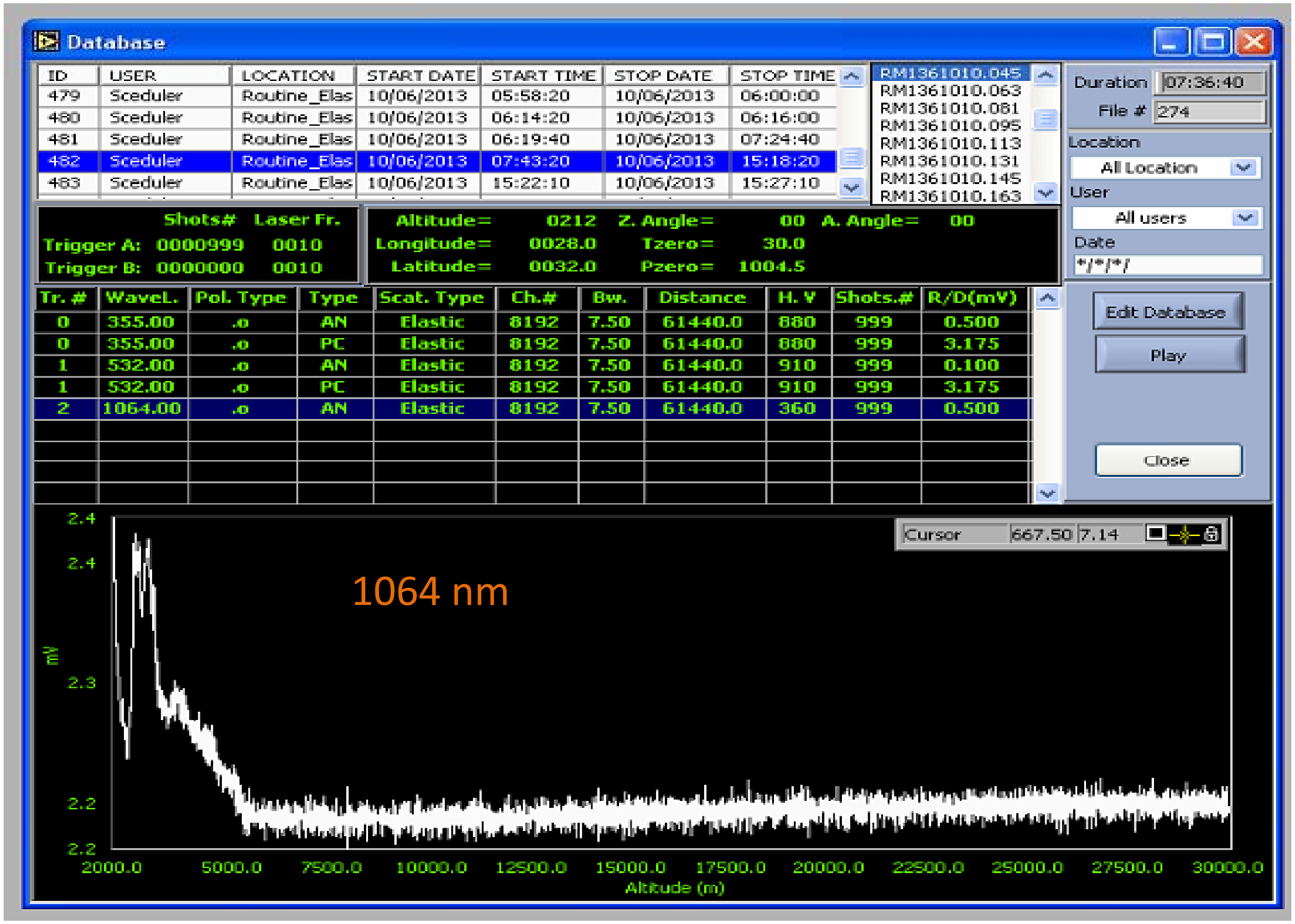

Problem due to not good earthing or too high HV

Examples (IV)

Raw lidar signal with dust layer

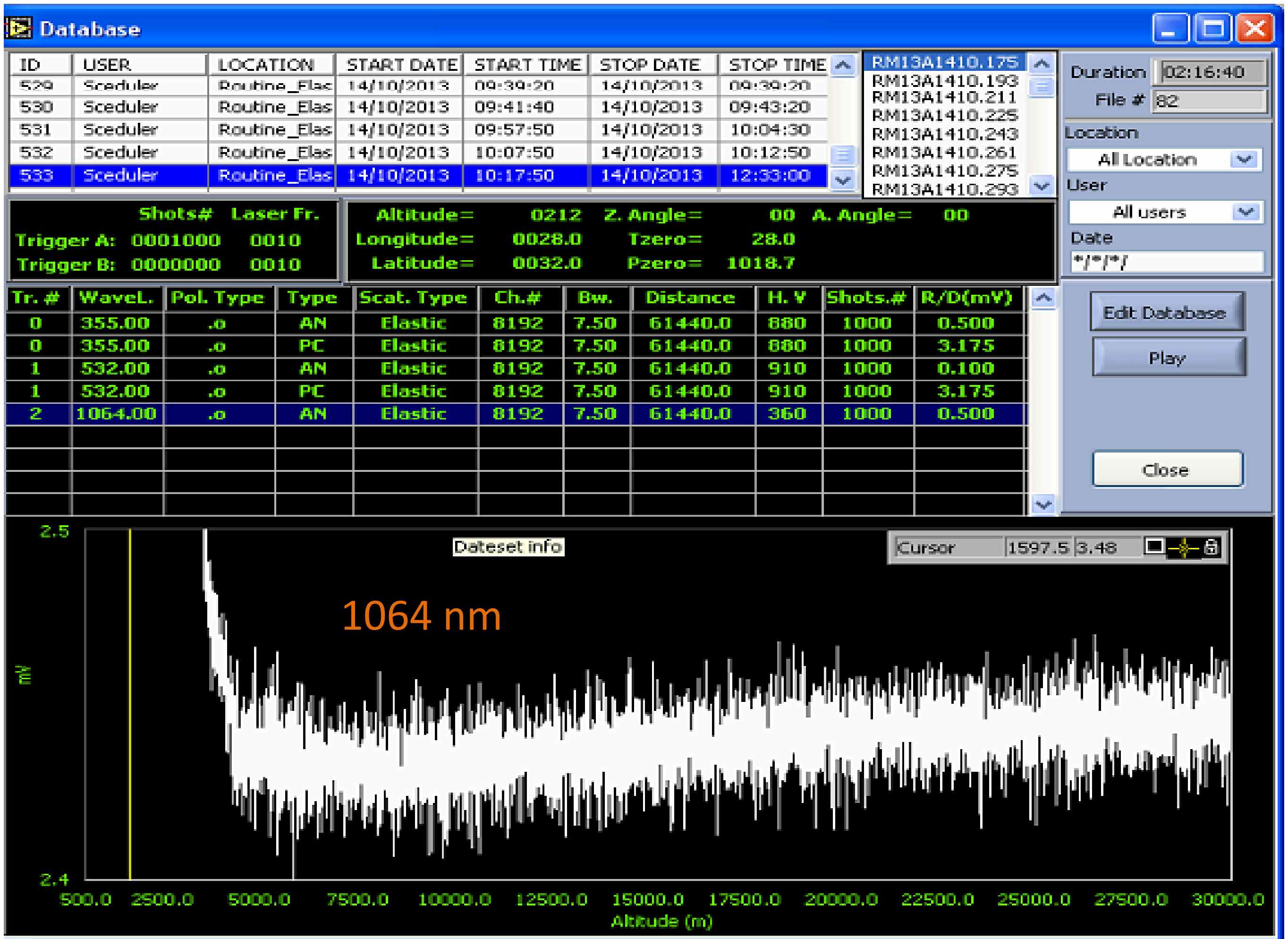

Problem due to not good earthing or too high HV

Examples (V)

Noise file (dark file)

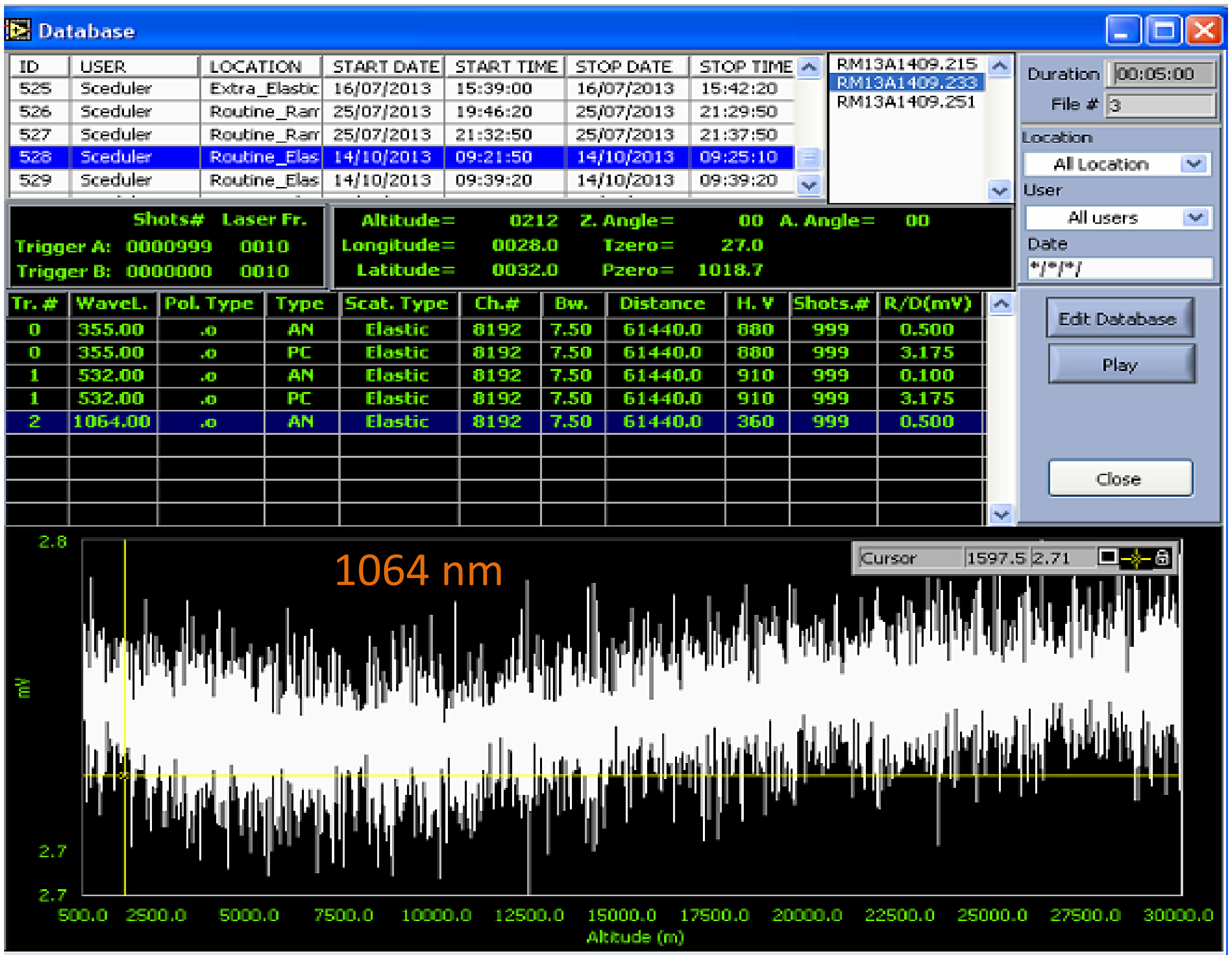

References – Books/Papers

Barbosa, H., et al., A permanent Raman lidar station in the Amazon: description, characterization and first results, Atmos. Meas. Tech., 7, 1745–1762, 2014.

Baudis, L., et al., Measurements of the position-dependent photo-detection sensitivity of the Hamamatsu R11410 and R8529 photomultiplier tubes, arXiv:1509.04055v1, 2015.

Evangelatos, C., P. Bakopoulos, G. Tsaknakis, D. Papadopoulos, G. Avdikos, A. Papayannis, G. Tzeremes, Continuous wave and passively Q-switched Nd:YAG laser with a multi-segmented crystal diode-pumped at 885 nm, Applied Optics, 52, 8795-8801, 2013.

Evangelatos, C., G. Tsaknakis, P. Bakopoulos, D. Papadopoulos, G. Avdikos, A. Papayannis, and G. Tzeremes, Q-switched laser with multi-segmented Nd:YAG crystal pumped at 885 nm for remote sensing, Photonics Technology Letters 26, 1890-1893, 2014.

Fiocco, G., and Smullin, L.D., Detection of scattering layers in the upper atmosphere by optical radar. Nature, **199**, 1275–1276, 1963.

Grath, A., et al., Injection-seeded single frequency, Q-switched Er:glass laser for remote sensing, Appl. Opt., 5706-5709, 1998.

Hulburt, E.O., Observations of a searchlight beam to an altitude of 28 kilometers. J. Opt. Soc. Am., **27**, 344-377, 1937.

Kokkalis, P., Study of the tropospheric aerosols using ground-based and space-borne techniques – Measurement analysis and statistical processing, Ph.D. Thesis (in Greek), NTUA, Greece, 2014.

Marcu, L., et a., Fluorescence Lifetime Spectroscopy and Imaging: Principles and Applications in Biomedical Diagnostics, 570 pp., CRC Press, 2014.

McGrath, A., Munch, J., Smith, G., Veitch, P., Injection-seeded, single frequency, Q-switched Er:glass laser for remote sensing, Appl. Opt., **37**, 5706-5709, 1998.

Measures, R. M.: Lidar Remote Sensing: Fundamentals and Applications, Krieger Publishing Company, Malabar, Florida, 2nd Edn., 1992.

Müller, J. W.: Dead-time problems, Nucl. Instrum. Methods, 112, 47–57, doi:10.1016/0029-554x(73)90773-8, 1973.

Newsom, R. K., Turner, D. D., Mielke, B., Clayton, M., Ferrare, R., and Sivaraman, C.: Simultaneous analog and photon counting detection for Raman lidar, Appl. Optics, 48, 3903–3914, doi:10.1364/AO.48.003903, 2009.

Siegman, A., Lasers, University Science Books, 1986.

Simeonov, V., et al., Influence of the photomultiplier tube spatial uniformity on lidar signals, Appl. Opt., 38, 5186-5190, 1999.

Stanford Research Systems. In Signal Recovery with Photomultiplier Tubes, Photon Counting, Lock-In Detection, or Boxcar Averaging?, Stanford Research Systems, AN 4, 15 pp., 1995.

References – Websites

www.hamamatsu.com

www.coherent.com

www.licel.com

www.olympusmicro.com

www.rp-photonics.com/beam_profilers.html